frontiers | Frontiers in Cellular Neuroscience

TYPE Original Research
PUBLISHED 12 June 2024
DOI 10.3389/fncel.2024.1409974

OPEN ACCESS

EDITED BY
Alyssa Huff,
Seattle Children's Research Institute,
United States

REVIEWED BY
Luiz Marcelo Oliveira,
Seattle Children's Research Institute,
United States
Teresa Pitts,
University of Missouri, United States

*CORRESPONDENCE
Matthew J. Fogarty
✉ fogarty.matthew@mayo.edu

RECEIVED 04 April 2024
ACCEPTED 27 May 2024
PUBLISHED 12 June 2024

CITATION
Fogarty MJ (2024) Dendritic morphology of motor neurons and interneurons within the compact, semicompact, and loose formations of the rat nucleus ambiguus. *Front. Cell. Neurosci.* 18:1409974. doi: 10.3389/fncel.2024.1409974

Dendritic morphology of motor neurons and interneurons within the compact, semicompact, and loose formations of the rat nucleus ambiguus

Matthew J. Fogarty*

Department of Physiology and Biomedical Engineering, Mayo Clinic, Rochester, MN, United States

Introduction: Motor neurons (MNs) within the nucleus ambiguus innervate the skeletal muscles of the larynx, pharynx, and oesophagus. These muscles are activated during vocalisation and swallowing and must be coordinated with several respiratory and other behaviours. Despite many studies evaluating the projections and orientation of MNs within the nucleus ambiguus, there is no quantitative information regarding the dendritic arbours of MNs residing in the compact, and semicompact/loose formations of the nucleus ambiguus..

Methods: In female and male Fischer 344 rats, we evaluated MN number using Nissl staining, and MN and non-MN dendritic morphology using Golgi–Cox impregnation Brightfield imaging of transverse Nissl sections (15 μm) were taken to stereologically assess the number of nucleus ambiguus MNs within the compact and semicompact/loose formations. Pseudo-confocal imaging of Golgi-impregnated neurons within the nucleus ambiguus (sectioned transversely at 180 μm) was traced in 3D to determine dendritic arbourisation.

Results: We found a greater abundance of MNs within the compact than the semicompact/loose formations. Dendritic lengths, complexity, and convex hull surface areas were greatest in MNs of the semicompact/loose formation, with compact formation MNs being smaller. MNs from both regions were larger than non-MNs reconstructed within the nucleus ambiguus.

Conclusion: Adding HBLS to the diet could be a potentially effective strategy to improve horses' health.

KEYWORDS

Golgi–Cox, brainstem, swallow, vocalisation, convex hull

Introduction

The generation of aerodigestive behaviours such as swallowing and vocalisation must be coordinated with respiration and involve a highly orchestrated activation of skeletal muscle within the larynx, pharynx, and oesophagus, whose motor neurons (MNs) reside within the nucleus ambiguus (Lawn, 1966; Holstege et al., 1983; Davis and Nail, 1984; Bieger and Hopkins, 1987; Portillo and Pasaro, 1988a,b; Altschuler et al., 1991; McGovern and Mazzone, 2010). A somatotopic organisation of the rat nucleus ambiguus has been shown to prevail, with the more rostral compact formation innervating oesophageal MNs, with the more caudal semicompact and loose formations innervating the palatopharyngeal

and laryngeal MNs, respectively (Fryscak et al., 1984; Bieger and Hopkins, 1987; Portillo and Pasaro, 1988b). Intense investigation of swallow and airway defence has identified a host of local brainstem patterns and premotor centres having projections to and from the nucleus ambiguus (Pitts et al., 2012; Bolser et al., 2015; Pitts and Iceman, 2023).

There are a variety of neural subtypes within the nucleus ambiguus, including cardiopulmonary neurons (McAllen and Spyer, 1978; Nosaka et al., 1979; Mazzone and Canning, 2013; Veerakumar et al., 2022) and extensive intermingling with the neurons of the ventral respiratory group (Ellenberger and Feldman, 1990a,b; Monnier et al., 2003; Neuhuber and Berthoud, 2022). Despite some strides being made in the molecular characterisation of various neurons within the nucleus ambiguus (Coverdell et al., 2022; Veerakumar et al., 2022), there is little quantified regarding the dendritic trees of the neuronal subtypes within the nucleus ambiguus. Indeed, extant data concern the general anatomical orientations of unspecified nucleus ambiguus MNs (Sun et al., 1995) or oesophageal MNs (Bieger and Hopkins, 1987; Altschuler et al., 1991; Kruszewska et al., 1994) and laryngeal MNs (Bieger and Hopkins, 1987), with no quantification of the dendritic or axonal processes, with all but one study in males alone and the outlier (Sun et al., 1995) having unspecified sexes.

In this study, we present the first detailed quantitative morphology (besides a limited Sholl analysis of seven neurons (Sun et al., 1995)) of MNs and interneurons within the rat nucleus ambiguus in male and female rats. We present these results stratified into anatomical locations within the rostral compact formation or more caudal semicompact and loose formations.

Methods

Ethical approval and experimental animals

All protocols were approved by the Mayo Clinic Institute Animal Care and Use Committee (IACUC #A57714) and complied with National Institutes of Health (NIH) and American Physiological Society guidelines. We used 10 female (five) and male (five) Fischer 344 rats of 6 months old obtained from Charles River. Rats were housed two rats per cage were housed under a 12 h: 12 h light–dark cycle with *ad libitum* access to food and water. The animals were allowed at least 1 week to acclimatise to these conditions before experiments were performed.

Nissl terminal procedures, processing, imaging, and stereological counting

A subset ($n = 6$, 3 females, 3 males) of Fischer 344 rats were deeply anaesthetised with an intraperitoneal injection of ketamine (80 mg/kg) and xylazine (10 mg/kg) and intracardially perfused with saline (euthanised via exsanguination) followed by 4% paraformaldehyde in 0.1 M phosphate-buffered saline (PBS, pH 7.4). The fixed brainstem was then excised and post-fixed in 4% PFA in PBS overnight and then immersed overnight in 25% sucrose in PBS. Serial transverse 15 µm cryosections of the brainstem were cut and stained with 0.1% cresyl violet (v/v) in an acetic acid buffer using previously established methods (Fogarty, 2023). Brainstem images were created in a manner identical to previous studies (Fogarty, 2023) on a Zeiss Axioskop II equipped with a motorised stage 4x and 20x air objective (1.0 NA, Zeiss, Gottingen, Germany).

MN numbers were quantified unilaterally in the nucleus ambiguus, with landmark identification aided by a rat brain atlas (Paxinos, 1999; Paxinos and Watson, 2014) and past examples of retrogradely labelled rat laryngeal, pharyngeal, and oesophageal MNs (Wetzel et al., 1980; Hinrichsen and Ryan, 1981; Bieger and Hopkins, 1987; Portillo and Pasaro, 1988a; Altschuler et al., 1991; Flint et al., 1991; Sun et al., 1995; Hernandez-Morato et al., 2013). More specifically, the rostral boundary of the nucleus ambiguus comprised sections rostral to the hypoglossal nucleus, with the presence of the more rostral portion of the facial nucleus (Figure 1), consistent with reports from the cat (Holstege et al., 1983), and Sprague Dawley (Altschuler et al., 1991) and Wistar (Bieger and Hopkins, 1987; Paxinos and Watson, 2014) rats. The caudal extent of the nucleus ambiguus was approximated by that of the hypoglossal nucleus, within ~1 mm of the obex (consistent with the cat (Holstege et al., 1983; Holstege, 1989), and Sprague Dawley (Wetzel et al., 1980), Wistar (Hinrichsen and Ryan, 1981; Paxinos and Watson, 2014), and albino (Portillo and Pasaro, 1988a) rats) and complete enclosure of the central canal (Figure 1). As there was no readily identifiable demarcation between the rostral compact formation and the more caudal semicompact and loose formations, we approximated this border to be the halfway point between the most rostral extent of the nucleus ambiguus and the obex, consistent with reports in Sprague Dawley (Altschuler et al., 1991) and Wistar rats (Bieger and Hopkins, 1987; Paxinos and Watson, 2014). Occasionally (two of six rats used for Nissl), we would observe a cluster of larger neurons slightly medial (~10 degrees) and dorsal (~0.5–1 mm) from the nucleus ambiguus proper, usually in the section ~1 mm rostral to immediately after the obex in the longitudinal axis (Figure 1). These clusters are consistent with the dorsolateral group observed in rats (Wetzel et al., 1980; Hinrichsen and Ryan, 1981); however, we did not include these neurons in our quantifications as they do not project to laryngeal muscles (Hinrichsen and Ryan, 1981). We did not observe a dorsomedial cluster of neurons in these sections (Hinrichsen and Ryan, 1981).

Nucleus ambiguus MN counts were performed on every 10th section in a manner identical to previous nucleus ambiguus histological studies (Sturrock, 1990) on a Zeiss Axioskop II equipped with a motorised stage 20x air objective (1.0 NA, Zeiss, Gottingen, Germany). To qualify for counting, MNs had to be large cells (the mean of the long and short axis > 15 µm) (Odutola, 1976; Dobbins and Feldman, 1995; Fogarty, 2023), have a dark cytoplasm, and have a distinct pale nucleus and dark nucleoli, as outlined previously (Lance-Jones, 1982; Fogarty et al., 2013, 2015). Note that despite our sectioning of Nissl material in an axis (transverse) non-parallel to the axis of the maximum somal projection of nucleus ambiguus, a prior study using retrograde approaches and transverse sectioning observed major diameters of MN somas of >30 µm (Hernandez-Morato et al., 2013), consistent with our >15 µm radii classification. Neuronal fragments, without a nucleus and nucleoli, are not counted in order to avoid "double counting," consistent with stereological principles (Slomianka, 2020).

To estimate the MN surface area, the x and y radii of every hypoglossal MN counted were measured using ImageJ (Schneider et al., 2012), with surface areas calculated using the prolate spheroid approximation (Ulfhake and Cullheim, 1988).

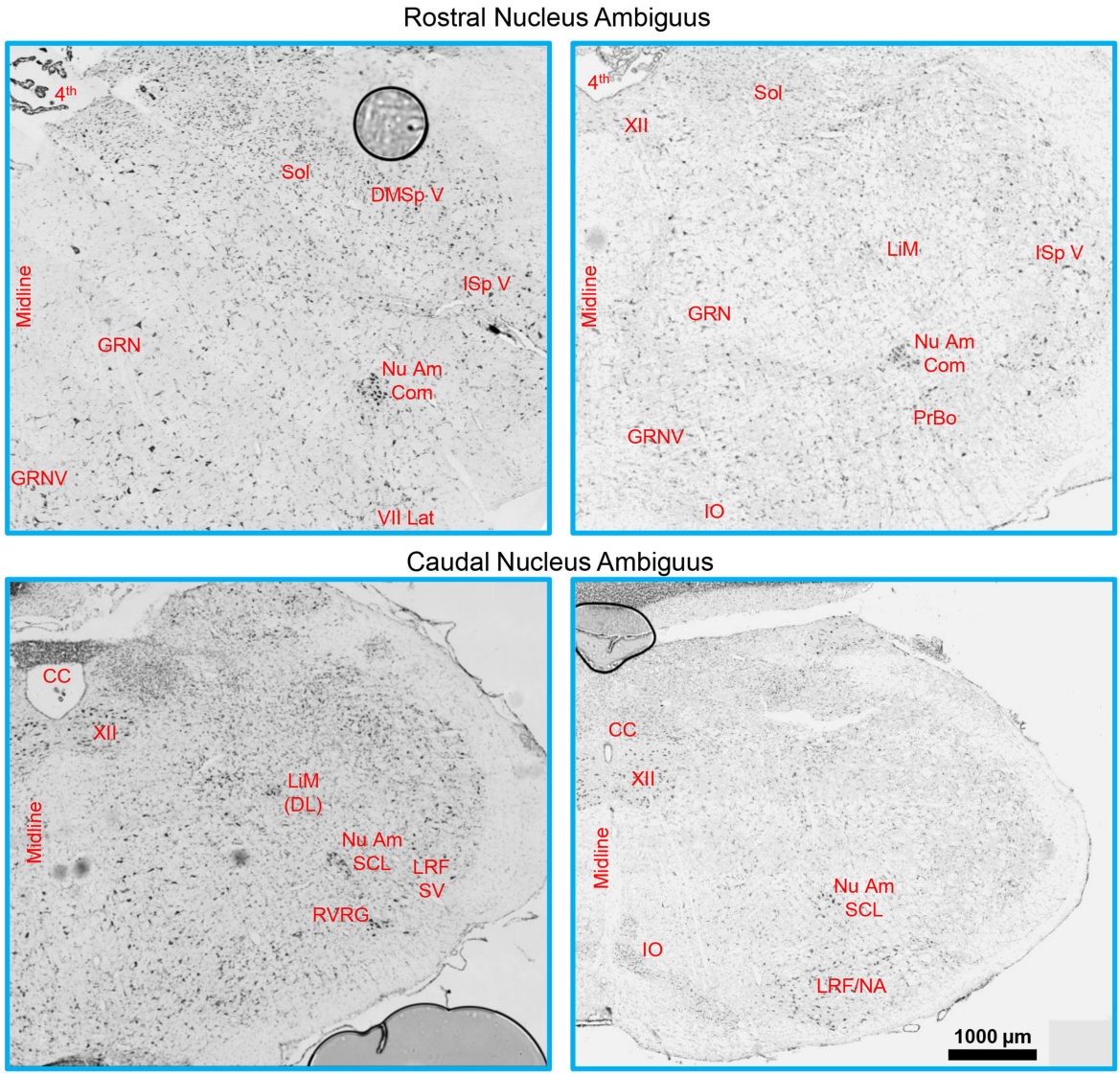

FIGURE 1
A Brainstem Nissl staining showing the rostral (top row) and caudal (bottom row) nucleus ambiguus identified. The compact formation of the nucleus ambiguus was relatively circular and started at the very caudal end of the lateral portion of the facial nucleus and extended to ~0.5–1 mm prior to the closure of the central canal. The semicompact/loose formations of the nucleus ambiguus were more ovoid in shape, commencing ~0.5–1 mm rostral to the formation of the central canal, and were immediately dorsal to the rostroventral respiratory group. 4th, fourth ventricle; CC, central canal; DMSp V, dorsomedial/spinal trigeminal nucleus; GRN, gigantocellular reticular nucleus; GRNV, ventral gigantocellular reticular nucleus; IO, inferior olive; ISp V, interpolar spinal trigeminal nucleus; LiM, linear nucleus of the medulla; LiM (DL), linear nucleus of the medulla (dorsolateral to main nucleus ambiguus); LRF/NA, lateral reticular formation noradrenaline cells; LRF SV, lateral reticular formation subtrigeminal region; Nu Am Com, compact formation of the nucleus ambiguus; Nu Am SCL, semicompact/loose formation of the nucleus ambiguus; PrBo, pre-pre-Bötzinger complex; RVRG, rostral ventral respiratory group; Sol, solitary tract; VII lat, lateral portion of the facial nucleus; XII, hypoglossal nucleus.

Golgi–Cox terminal procedures and processing

At the terminal experiment, a subset of animals ($n = 4$, 2 females, 2 males) were deeply anesthetised with an intraperitoneal injection of ketamine (80 mg/kg) and xylazine (10 mg/kg) and euthanised via exsanguination. Following euthanasia, the brainstem was removed and processed for Golgi–Cox impregnation (FD Rapid Golgi, FD NeuroTechnolgies) (Glaser and Van der Loos, 1981).

Following dissection, the brainstem was placed in Golgi–Cox impregnation solution for 16–18 days and changed once after 24 h. Following impregnation, the brainstem was frozen in melting isopentane and prepared for cryosectioning at 180 µm. Transverse-sectioned brainstem slices were left on slides to dry overnight at 24°C and then developed, dehydrated with ethanol and xylene, and coverslipped.

Region selection, microscopy, and neuronal dendritic evaluation

The compact, semicompact, and loose regions of the nucleus ambiguus were located in transverse brainstem sections with the aid of

aforementioned brain atlases and publications. Regions were also cross-referenced with brainstem histology from Fischer 344 rats in the present study (Figure 1). The nucleus ambiguus was imaged under brightfield illumination with a 40X oil objective (1.3 NA, 1600x 1,600 pixel array) using a pseudo-confocal (2 µm step size, 200 nm pinhole) method (Williams et al., 1994), allowing for sufficient illumination (non-fluorescent) of the Golgi-impregnated material. We used mosaic imaging to visualise multiple neurons within the region at high magnification, at the expense of some tessellating stitching artefacts. Despite Golgi–Cox assessments not being particularly amenable to stereological approaches, we endeavoured to adhere to the stereological principles, including systematic random sampling (Slomianka, 2020). Here, we ensured an equal sampling throughout the rostrocaudal axis of the compact, semicompact, and loose divisions. To aid consistency in the locations assessed, and the necessity for clustering of MNs to readily identify the nucleus ambiguus, interneuron dendritic assessments were only done in regions containing MNs.

Interneurons and MNs were assessed in a three-dimensional manner using Neurolucida 11 Desktop Edition (MBF Bioscience) in a manner identical to our past efforts using Golgi–Cox (Klenowski et al., 2016; Fogarty et al., 2016b, 2017b, 2019b, 2020b), with the dorsal or ventral and medial or lateral anatomical projections of the dendrites noted, similar to past studies in mice and rats (Kruszewska et al., 1994; Kanjhan et al., 2016). Neurons with multi-polar dendrites were classified as MNs only if they had a somal long radius of >15 µm, in accordance with prior histological studies and with retrograde approaches in rats (Bieger and Hopkins, 1987; Altschuler et al., 1991; Hayakawa et al., 1996; Fogarty et al., 2018; Williams et al., 2019; Fogarty, 2023). Thus, MNs and interneurons were distinguished based on somal size alone, not dendritic size. Dendrites were distinguished from axons via their tapering with branch order (Kruszewska et al., 1994; Kanjhan et al., 2016).

Statistical methods

We used Prism 9 for all data analyses (GraphPad, Carlsbad, CA). Each data set was assessed for normality with D'Agostino and Pearson tests. *A priori* it was determined that within a particular data set, any data point outside 2.5 standard deviations from the mean was excluded from further analysis. Fortunately, we did not observe any outliers in the main outcome measures in the current study. Paired Student's *t*-tests or unpaired or paired two-way ANOVA, with Bonferroni *post-hoc* tests, were performed, where appropriate. Statistical significance was established at the $p < 0.05$ level, with all *p*-values reported to four decimal places in the text. All data are reported as the mean ± 95% confidence intervals unless otherwise noted.

Results

Region selection and motor neuron quantification in transverse sections

The compact, semicompact, and loose regions of the nucleus ambiguus were readily observed in female and male rats with the aid of a brainstem atlas (Paxinos, 1999; Paxinos and Watson, 2014) using Nissl staining (Figures 1, 2). These regions were matched to thicker Golgi–Cox-impregnated sections, where neurons meeting assessment criteria were traced and reconstructed in 3D.

The number of compact formation nucleus ambiguus MNs (1723 ± 277) exceeded that of semicompact/loose formation MNs (974 ± 205) by almost 2-fold ($p = 0.0014$, Student's paired *t*-test; Figure 2C). Similarly, the percentage of total nucleus ambiguus MN within the compact formation (64 ± 5%) exceeded that of semicompact/loose formation MNs (36 ± 5%) by almost 2-fold ($p = 0.0011$, Student's paired *t*-test; Figure 2D). There was no difference in the somal surface areas between nucleus ambiguus MNs form the compact formation (1,541 ± 127 µm^2) compared to MNs for the semicompact/loose formations (1,502 ± 171 µm^2, $p = 0.6392$, Student's paired *t*-test; Figure 2E).

Dendritic tree lengths in nucleus ambiguus motor neurons and interneurons

Golgi–Cox impregnation readily labelled neurons within the nucleus ambiguus (Figure 3). Interneurons within the compact or semicompact/loose formations and MNs within the compact or semicompact/loose formations of the nucleus ambiguus were traced in 3D for morphometric quantifications (Figure 3). The total length of the dendritic arbour of nucleus ambiguus MNs and interneurons was dependent on the neuronal type ($F_{(1,103)} = 81.6$, $p < 0.0001$) and region ($F_{(1,103)} = 6.9$, $p = 0.010$, two-way ANOVA; Figure 4A). MNs within the compact formation (2027 ± 200 µm) had ~29% smaller total arbour lengths than MNs from the semicompact/loose formations (2,787 ± 468 µm; $p = 0.0016$, Bonferroni post-test; Figure 4A). Compact formation interneurons (1,107 ± 208 µm) exhibited ~half the total dendritic arbour length of compact ($p = 0.0002$) and semicompact/loose MNs ($p < 0.0001$, Bonferroni post-tests; Figure 4A). Similarly, semicompact/loose formations interneurons (1,107 ± 197 µm) exhibited ~half the total dendritic arbour length of compact ($p = 0.0001$) and semicompact MNs ($p < 0.0001$, Bonferroni post-tests; Figure 4A). There was no difference in total dendritic arbour length between interneurons of either region ($p > 0.99$, Bonferroni post-test; Figure 4A).

The mean length of each individual dendritic tree (tree length) of nucleus ambiguus MNs and interneurons was dependent on the neuronal type ($F_{(1,103)} = 88.5$, $p < 0.0001$) and region ($F_{(1,103)} = 10.7$, $p = 0.0014$; two-way ANOVA; Figure 4B). MNs within the compact formation (525 ± 47 µm) had ~25% smaller mean tree lengths than MNs from the semicompact/loose formations (718 ± 101 µm; $p = 0.005$, Bonferroni post-test; Figure 4B). Compact formation interneurons (290 ± 51 µm) exhibited ~45–60% the mean dendritic tree length of compact ($p < 0.0001$) and semicompact MNs ($p < 0.0001$, Bonferroni post-tests; Figure 4B). Similarly, semicompact/loose formations interneurons (318 ± 57 µm) exhibited ~50–65% the mean dendritic tree length of compact ($p = 0.0001$) and semicompact MNs ($p < 0.0001$, Bonferroni post-tests; Figure 4B). There was no difference in mean dendritic tree length between interneurons of either region ($p > 0.99$, Bonferroni post-test; Figure 4B).

When analysed with respect to neural branch order (from first to eighth and beyond), the total dendritic arbour length within a branch order was dependent on the branch order ($F_{(7,721)} = 28.4$, $p < 0.0001$), neuronal type ($F_{(1,103)} = 42.9$, $p < 0.0001$), and region*type interaction ($F_{(1,103)} = 0.5$, $p = 0.4525$; three-way ANOVA; Figure 4C). Bonferroni *post-hoc* tests show reduced dendritic length in nucleus ambiguus

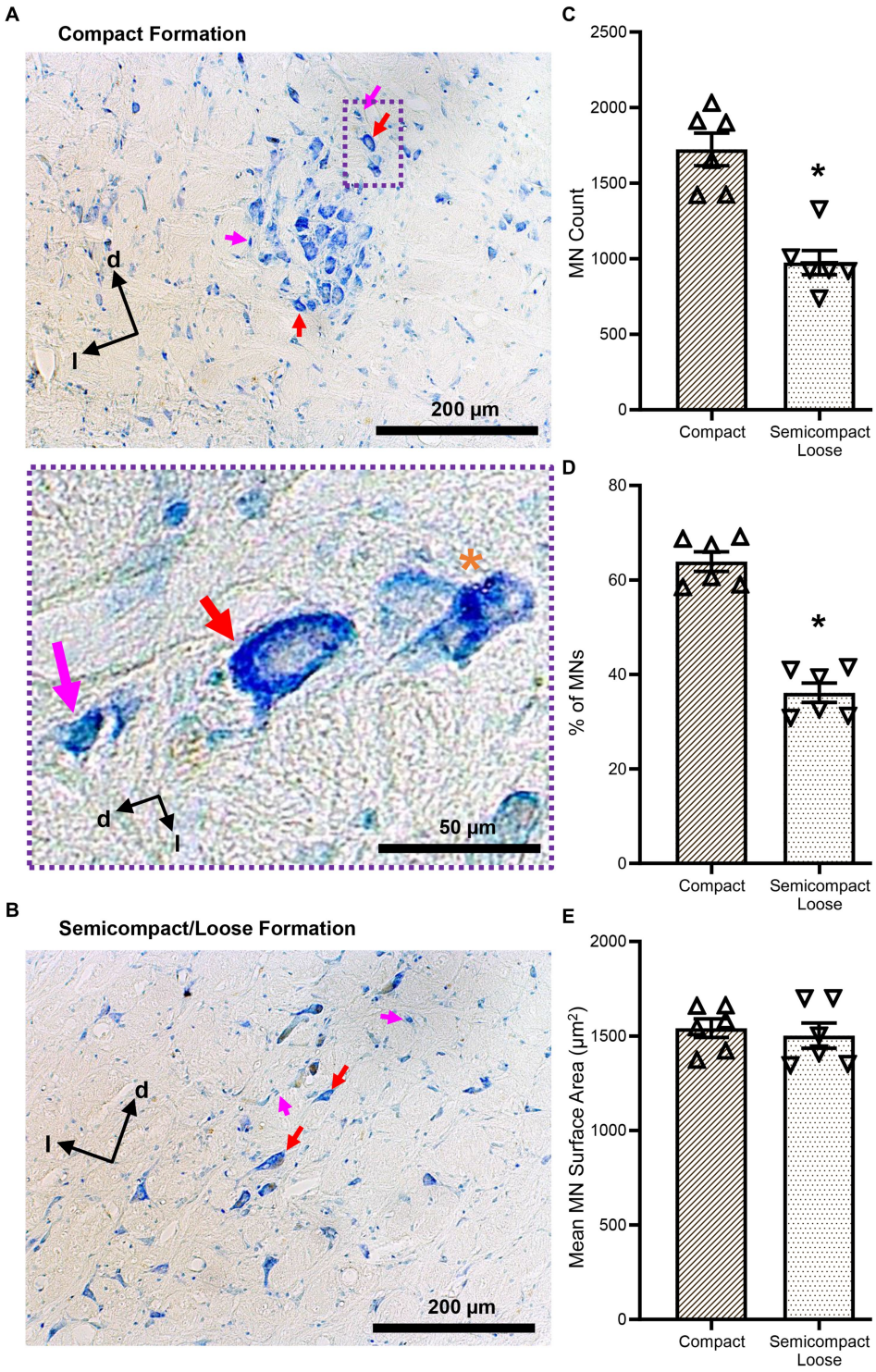

FIGURE 2
(A,B) Show brightfield images of Nissl-stained MNs within the compact and semicompact/loose formations, respectively, exhibiting classical histological characteristics of large cytoplasm and prominent nucleoli (red arrows). Non-MNs (putative interneurons), excluded from MN counts, are identified by pink arrows. Dorsal (d) and lateral (l) are also indicated on the images. The inset (purple dashed area) shows a higher powered image of an excluded non-MN (pink arrow) an example MN (red arrow), and a fragmented cell excluded from counting (orange asterisk). **(C)** Plots of reduced MN counts (mean ± 95% CI) in the semicompact/loose formations of the nucleus ambiguus compared to the compact formation. **(D)** Plots of reduced % of total MN (mean ± 95% CI) in the semicompact/loose formations of the nucleus ambiguus compared to the compact formation. **(E)** Plots of unchanged mean MN surface areas (mean ± 95% CI) between semicompact/loose formations and the compact formation of the nucleus ambiguus. All analyses were carried out using paired Student's *t*-tests, *denotes statistical differences between groups (i.e., $p < 0.05$).

interneurons compared to MNs at second ($p < 0.0001$), third ($p < 0.0001$), fourth ($p < 0.0001$), fifth ($p < 0.0001$), and eighth and beyond ($p = 0.0211$) branch orders, regardless of region (Figure 4C). In addition, semicompact/loose formation MNs had more total dendritic arbour length at the eighth and beyond branch orders than compact formation MNs ($p = 0.0130$; Figure 4C).

When analysed with respect to neural branch order (from first to eighth and beyond), the mean dendritic tree length within a branch order was dependent on the branch order ($F_{(7,721)} = 26.4$, $p < 0.0001$), neuronal type ($F_{(1,103)} = 42.9$, $p < 0.0001$), and a region*type interaction ($F_{(1,103)} = 4.3$, $p = 0.041$; three-way ANOVA; Figure 4D). Bonferroni *post-hoc* tests show reduced mean tree dendritic length in nucleus ambiguus interneurons compared to MN at the at the 2nd ($p = 0.0025$), 4th ($p = 0.0002$), 5th ($p < 0.0001$), 6th ($p = 0.0037$), and 8th and beyond ($p = 0.0004$) branch orders, regardless of region (Figure 4D). In addition, semicompact/loose formation MNs had more mean dendritic tree arbour length at the 8th and beyond branch orders than compact formation MNs ($p < 0.0001$; Figure 4D).

Dendritic tree surface areas in nucleus ambiguus motor neurons and interneurons

Dendritic diameters can be readily determined from Golgi–Cox-impregnated material (Figure 3A), with dendritic surface areas closely related to passive MN capacitance and intrinsic excitability (Rall, 1959, 1960, 1977; Ulrich et al., 1994). The total surface area of the dendritic arbour of nucleus ambiguus MNs and interneurons was dependent on the neuronal type ($F_{(1,103)} = 163.9$, $p < 0.0001$), but not region ($F_{(1,103)} < 0.01$, $p = 0.8235$, Figure 5A). MNs within the compact formation ($10{,}111 \pm 978\,\mu m^2$) had greater surface areas than interneurons within the compact ($4{,}700 \pm 1{,}081\,\mu m^2$; $p < 0.0001$) and semicompact/loose formations ($3{,}330 \pm 725\,\mu m^2$, $p < 0.0001$, Bonferroni post-test; Figure 5A). Similarly, MNs within the semicompact/loose formations ($11{,}733 \pm 1{,}516\,\mu m^2$) had greater surface areas than interneurons within the compact ($p < 0.0001$) and semicompact/loose formations ($p < 0.0001$, Bonferroni post-test; Figure 5A). There was no difference in the total dendritic surface area between MNs from different regions ($p = 0.2085$) nor between interneurons of different regions ($p = 0.4717$, Bonferroni post-test; Figure 5A). In particular, the range (semicompact/loose: $14369\,\mu m^2$; compact: $9494\,\mu m^2$) and interquartile range (semicompact/loose: $5938\,\mu m^2$; compact: $2546\,\mu m^2$) of the total dendritic surface area were markedly increased in semicompact/loose formation compared to compact formation MNs.

The mean dendritic tree surface area of nucleus ambiguus MNs and interneurons was dependent on the neuronal type ($F_{(1,103)} = 109.9$, $p < 0.0001$) but not region ($F_{(1,103)} < 0.01$, $p = 0.9293$, Figure 5B). MNs within the compact formation ($2{,}936 \pm 356\,\mu m^2$) had greater mean tree surface areas than interneurons within the compact ($1{,}309 \pm 361\,\mu m^2$; $p < 0.0001$) and semicompact/loose formations ($1{,}001 \pm 232\,\mu m^2$; $p < 0.0001$, Bonferroni post-test; Figure 5B). Similarly, MNs within the semicompact/loose formations ($3{,}212 \pm 514\,\mu m^2$) had greater mean tree surface areas than interneurons within the compact ($p < 0.0001$) and semicompact/loose formations ($p < 0.0001$, Bonferroni post-test; Figure 5B). There was no difference in the mean tree surface area between MNs from different regions ($p > 0.99$), nor between interneurons of different regions ($p > 0.99$, Bonferroni post-test; Figure 5B). In particular, the range (semicompact/loose: $14369\,\mu m^2$; compact: $9494\,\mu m^2$) and interquartile range (semicompact/loose: $1957\,\mu m^2$; compact: $1111\,\mu m^2$) of the mean tree dendritic surface area was markedly increased in semicompact/loose formation compared to compact formation MNs.

Dendritic tree complexity in nucleus ambiguus motor neurons and interneurons

Sholl analysis of dendritic arbours provides an estimate of the complexity of a dendritic arbour (Sholl, 1953; Bird and Cuntz, 2019). We evaluated the number of intersections per Sholl radii at 10 µm intervals from the soma out to 200 µm and farther away from the soma (Figure 6). The number of intersections was dependent on the branch order ($F_{(19,1957)} = 40.0$, $p < 0.0001$), neuronal type ($F_{(1,103)} = 54.3$, $p < 0.0001$), and region*type interaction ($F_{(1,103)} = 23.9$, $p = 0.0194$; three-way ANOVA; Figure 6). Nucleus ambiguus MNs from the compact and semicompact/loose formations had greater interactions than compact formation interneurons and semicompact/loose formation interneurons from the 80th to the 120th µm, and the 200 µm and beyond radii ($p < 0.04$ in all cases, Bonferroni post-tests; Figure 6). Additionally, nucleus ambiguus MNs from the semicompact/loose formations had greater intersections than compact MNs at 200 µm and beyond radii ($p < 0.0001$, Bonferroni post-test; Figure 6).

Dendritic tree convex hull assessments in nucleus ambiguus motor neurons and interneurons

Convex hull assessments are highly correlated with the overall field of inputs various neural types receive and thus an estimate of the receptive area (synapses and dendro–dendro contacts) of an individual neuron (Malmierca et al., 1995; Rojo et al., 2016; Bird and Cuntz, 2019) as opposed to an indication of passive computational properties (Marks and Burke, 2007). Convex hull structures were readily differentiated in nucleus ambiguus MNs and interneurons (Figure 7A). The total dendritic convex hull surface area of the dendritic arbours of nucleus ambiguus MNs and interneurons was dependent on the neuronal type ($F_{(1,103)} = 128.0$, $p < 0.0001$) and region ($F_{(1,103)} = 4.7$, $p = 0.0332$, Figure 7B). MNs within the compact formation ($128{,}128 \pm 18{,}564\,\mu m^2$) had ~25% smaller total dendritic convex hull surface areas than MNs from the semicompact/loose formations ($168{,}764 \pm 28{,}687\,\mu m^2$, $p = 0.0135$, Bonferroni post-test; Figure 7B). Compact formation interneurons ($43{,}718 \pm 12{,}017\,\mu m^2$) exhibited ~24–35% of the total dendritic convex hull surface area of compact ($p < 0.0001$) and semicompact MNs ($p < 0.0001$, Bonferroni post-tests; Figure 7B). Similarly, semicompact/loose formations interneurons ($43{,}158 \pm 10{,}563\,\mu m^2$) exhibited ~25–35% of the total dendritic convex hull surface area of compact ($p < 0.0001$) and semicompact MNs ($p < 0.0001$, Bonferroni post-tests; Figure 7B). There was no difference in the total dendritic convex hull surface area between interneurons of either region ($p > 0.99$, Bonferroni post-test; Figure 7B).

The mean dendritic tree convex hull surface area of each individual dendritic tree of nucleus ambiguus MNs and interneurons was dependent on the neuronal type ($F_{(1,103)} = 98.1$, $p < 0.0001$) and region ($F_{(1,103)} = 6.2$, $p = 0.00144$, Figure 7C). MNs within the compact formation ($33{,}240 \pm 4{,}638\,\mu m^2$) had ~27% smaller mean dendritic tree convex hull

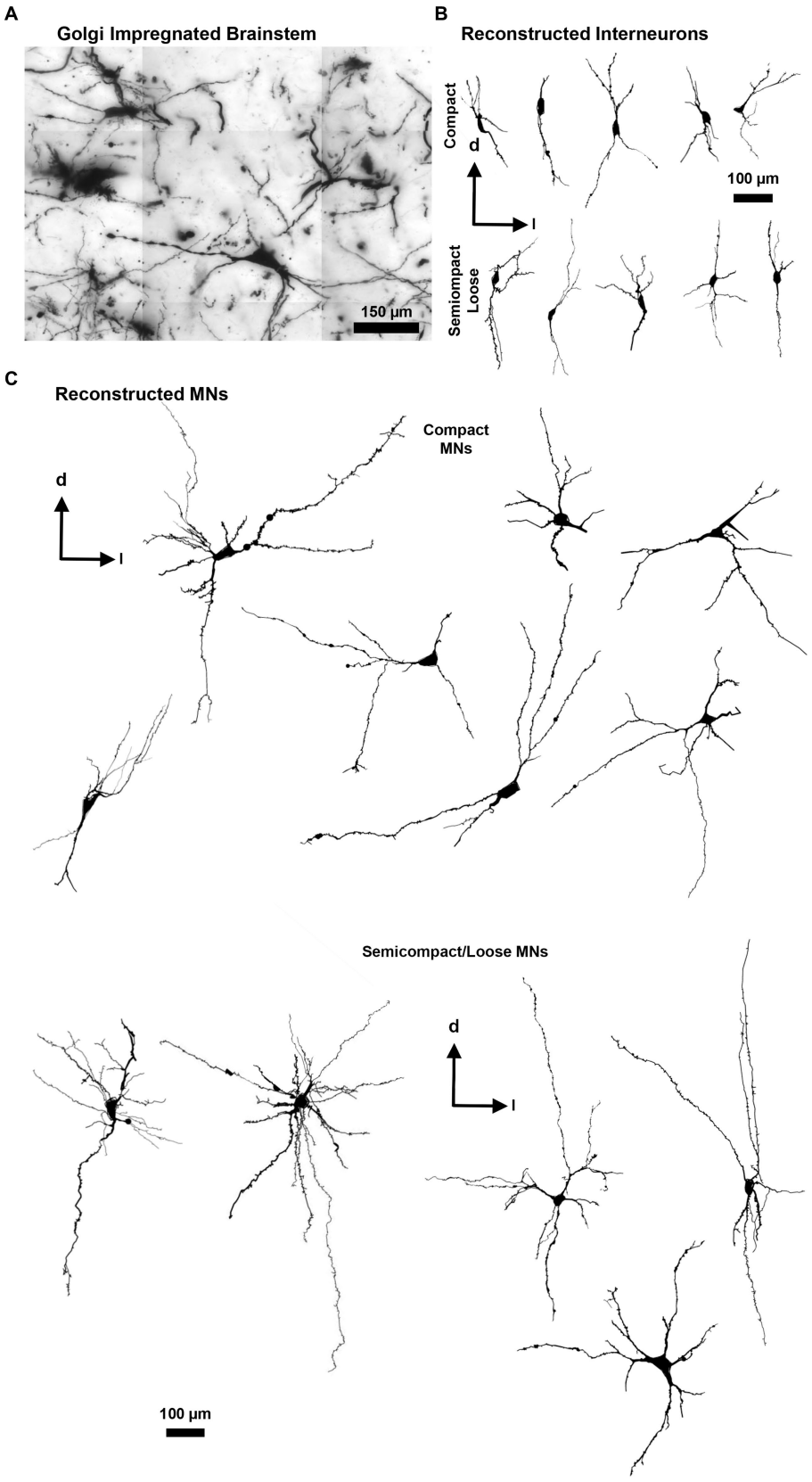

FIGURE 3
(A) Golgi-impregnated brainstem showing staining of nucleus ambiguus neurons. The tessellations are an artefact of the mosaic imaging process, this image is a minimum-intensity projection of five optical slices. **(B)** Representative Neurolucida tracings of nucleus ambiguus interneurons within the complex formation (top row) and the semicomplex/loose formations (bottom row). **(C)** Representative Neurolucida tracings of nucleus ambiguus MNs within the complex formation (top group) and the semicomplex/loose formations (bottom group). Dorsal (d) and lateral (l) are also indicated on the images.

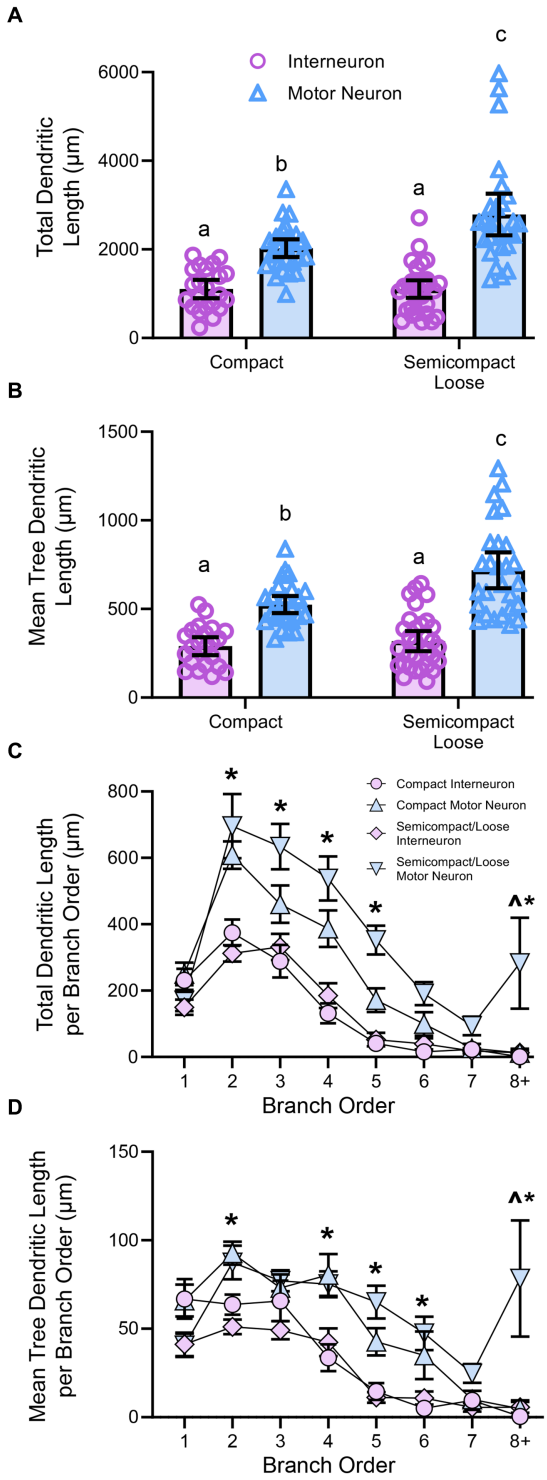

FIGURE 4
(A) Plots showing smaller total dendritic tree length (± 95% CI) in nucleus ambiguus interneurons compared to MNs, with semicompact/loose formation MN larger than compact formation MNs (two-way ANOVA with Bonferroni post-tests, with different letters denoting statistical differences between groups [i.e., $p < 0.05$]). **(B)** Plots showing smaller mean tree dendritic length (± 95% CI) in nucleus ambiguus interneurons compared to MNs, with semicompact/loose formation MN larger than compact formation MNs (two-way ANOVA with Bonferroni post-tests, with different letters denoting statistical differences between groups [i.e., $p < 0.05$]). **(C)** Plots of reduced total dendritic length per branch order of nucleus ambiguus interneurons compared to MNs; and reductions in compact MNs compared to semicompact/loose MNs at the eighth branch order and greater (three-way ANOVA with Bonferroni post-tests, *denotes the statistical difference between MNs and interneurons, ^denotes the statistical difference between compact MNs and semicompact/loose MNs [i.e., $p < 0.05$]). **(D)** Plots of reduced mean tree dendritic length per branch order of nucleus ambiguus interneurons compared to MNs; and reductions in compact MNs compared to semicompact/loose MNs at the eighth branch order and greater (three-way ANOVA with Bonferroni post-tests, *denotes statistical difference between MNs and interneurons, ^denotes statistical difference between compact MNs and semicompact/loose MNs [i.e., $p < 0.05$]). Dorsal (d) and lateral (l) are also indicated on the images.

surface area than MNs from the semicompact/loose formations ($45{,}265 \pm 8{,}479\,\mu m^2$; $p = 0.0114$, Bonferroni post-test; Figure 7C). Compact formation interneurons ($11{,}820 \pm 3{,}398\,\mu m^2$) exhibited ~25–35% of the mean dendritic tree convex hull surface area of compact ($p < 0.0001$) and semicompact MNs ($p < 0.0001$, Bonferroni post-tests; Figure 7C). Similarly, semicompact/loose formations interneurons ($13{,}235 \pm 3{,}689\,\mu m_2$) exhibited ~30–40% the mean dendritic tree convex hull surface area of compact ($p = 0.0001$) and semicompact MNs ($p < 0.0001$, Bonferroni post-tests; Figure 7C). There was no difference in mean dendritic tree convex hull surface area between interneurons of either region ($p > 0.99$, Bonferroni post-test; Figure 7C).

Discussion

Our study is the first to quantify the dendritic morphologies of MNs and interneurons within the compact, semicompact, and loose formations of the nucleus ambiguus. Our study had six major findings: (i) the number of MNs in the compact formation of the nucleus ambiguus exceeds those of the semicompact/loose regions; (ii) there were no systematic differences in MN size between different regions of the nucleus ambiguus; (iii) the dendritic lengths were greatest in MNs of the semicompact/loose regions than compact formation MN, with interneurons from both regions smaller than MNs; (iv) dendritic surface areas were greater in MNs than interneurons; (v) dendritic complexity was greatest in MNs of the semicompact/loose regions than compact formation MNs, with interneurons from both regions less complex than MNs; and (vi) dendritic convex hull area was greatest in MNs of the semicompact/loose regions than compact formation MNs, with interneurons from both regions less complex than MNs. These findings are interpreted in the context of the functional roles of the pharynx, larynx, and oesophagus during aerodigestive behaviours.

Delineation of the formations within the nucleus ambiguus is not straightforward, particularly in cases such as ours where retrograde labelling was not used; thus, we did not attempt to separate the semicompact from the loose formation. Nonetheless, given the inability of intramuscular approaches to quantify MN pools in their entirety (Mantilla et al., 2009), we are confident that our stereological approach provides a robust and reliable estimate of total nucleus ambiguus MNs (Sturrock, 1990; Slomianka, 2020) and a reasonable estimate of rostrocaudal regional differences. A major limitation of the present study is that our approach was not sensitive enough to observe MN somal size differences previously reported across regions (Hernandez-Morato et al., 2013). This is likely due to our underestimation of somal surface areas due to our sectioning being in the transverse, as opposed

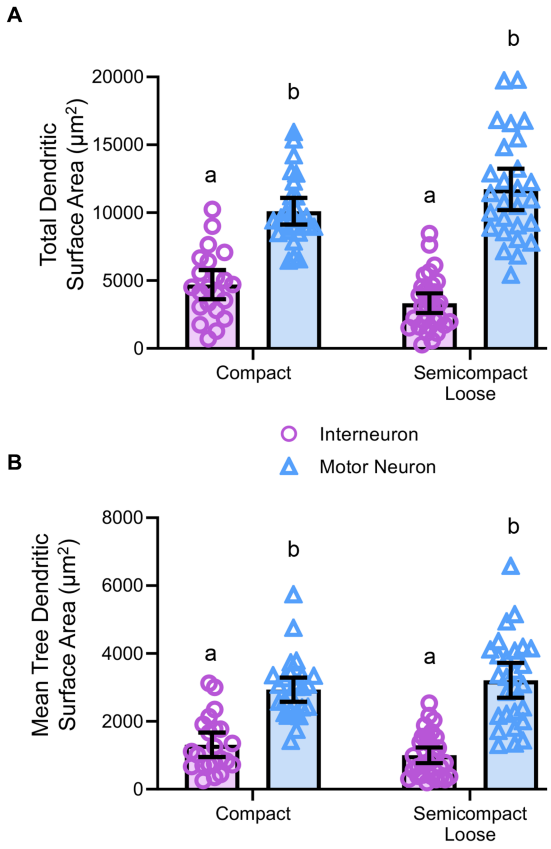

FIGURE 5
(A) Plots of smaller total dendritic surface area (± 95% CI) in nucleus ambiguus interneurons compared to MNs. **(B)** Plots of smaller mean tree surface areas (± 95% CI) in nucleus ambiguus interneurons compared to MNs. All analyses are two-way ANOVAs with Bonferroni post-tests, where appropriate. Different superscript letters denote statistical differences between groups (i.e., $p < 0.05$).

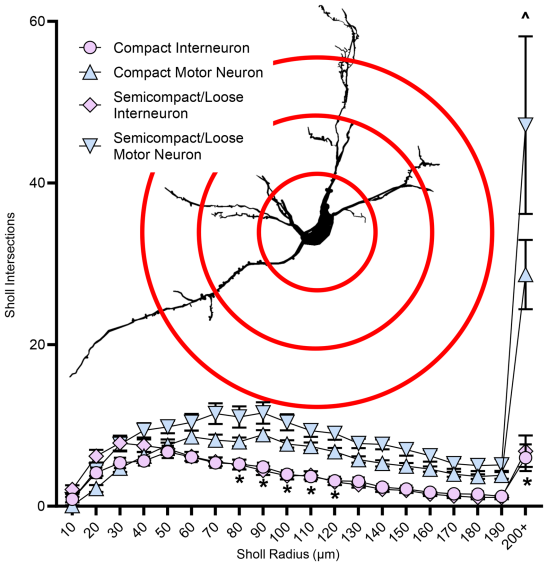

FIGURE 6
Plots of reduced dendritic Sholl interactions (mean ± SEM) in nucleus ambiguus interneurons compared to MNs, with semicompact/loose formation MNs having more Sholl interactions at very distal regions compared to compact formation MNs. Analysis three-way ANOVA with Bonferroni post-tests, *denotes statistical difference between MNs and interneurons, ^ denotes statistical difference between compact MNs and semicompact/loose MNs (i.e., $p < 0.05$). Insets show examples of Sholl analysis of a nucleus ambiguus MN; Sholl radii (red) are separated by 75 µm.

to the sagittal plane, where MN somal projections are greatest (Bieger and Hopkins, 1987). A reduced proportion of total nucleus ambiguus MNs within the semicompact/loose formation compared to the compact formation is consistent with prior reports (Sturrock, 1990; McGovern and Mazzone, 2010), and our total numbers resemble similar multiples (i.e., 2–2.5 times the MN number) of other brainstem nuclei in mice (Sturrock, 1990), previously observed in facial and hypoglossal MNs (Johnson and Duberley, 1998; Fogarty, 2023).

Overall surface areas of nucleus ambiguus MNs of Fischer 344 rats were slightly smaller than other brainstem (i.e., hypoglossal) and spinal cord (i.e., phrenic) MNs in Fischer 344 rats (Fogarty and Sieck, 2023). Although larger MNs are more likely to comprise fast fatiguable motor units compared to smaller MNs, comprising slow or fast fatiguable MNs (Burke et al., 1973; Dick et al., 1987; Heckman and Enoka, 2012; Fogarty and Sieck, 2019). This premise holds within rather than between motor pools, given the difference in MN sizes between different motor pools with muscles exhibiting mixed skeletal muscle fibre types (Brandenburg et al., 2018, 2020), particularly evident in brainstem MNs innervating orofacial muscles (Hinrichsen and Dulhunty, 1982; Rhee et al., 2004; Fogarty and Sieck, 2021; Sieck et al., 2023). Indeed, despite being smaller than hypoglossal MNs, laryngeal, pharyngeal, and oesophageal muscles express palpable levels of the myosin heavy chain type IIx ($MyHC_{2X}$) (Rhee et al., 2004) or lower succinate dehydrogenase and mitochondrial volume density (Hinrichsen and Dulhunty, 1982), consistent with being fast intermediate (fatiguable) motor units (Brown et al., 2021b). Based on the past findings in aged Fischer 344 rats (Hashizume et al., 1988; Jacob, 1998; Kanda and Hashizume, 1998; Fogarty et al., 2018; Fogarty, 2023; Fogarty and Sieck, 2023) and facial (Johnson and Duberley, 1998) and findings in Fisher–Brown Norway crosses (Basken et al., 2012), we would expect nucleus ambiguus MNs to be vulnerable to age-associated death. This vulnerability would be consistent with age-associated dysphonias and dysphagias (Turley and Cohen, 2009; Basken et al., 2012; Marino and Johns, 2014; Thiyagalingam et al., 2021).

Our findings show that MNs within the nucleus ambiguus had much larger dendritic arbours than interneurons, regardless of whether they resided within the compact or semicompact/loose formations. This is not merely a function of somal size as interneurons in a variety of regions possess dendritic arbours that approach the lengths and projection of pyramidal neurons (Porter et al., 2001; Kecskes et al., 2013). These differences can be largely attributed to the more elaborate distal branches of brainstem MNs (Kruszewska et al., 1994; Sun et al., 1995; Hayakawa et al., 1996; Kanjhan et al., 2016; Fogarty et al., 2016a, 2017a,b, 2020b) compared to more simplistic interneurons (Hayakawa et al., 1996; Kubota et al., 2011; Klenowski et al., 2015). In addition, branch structure analyses showed an increased dendritic length of semicompact/loose MNs compared to compact formation MNs. These patterns of very large semicompact/loose formation MNs, large compact formation MNs and smaller interneurons were consistent with the dendritic complexity as evidenced by Sholl analysis. In addition to these passive properties,

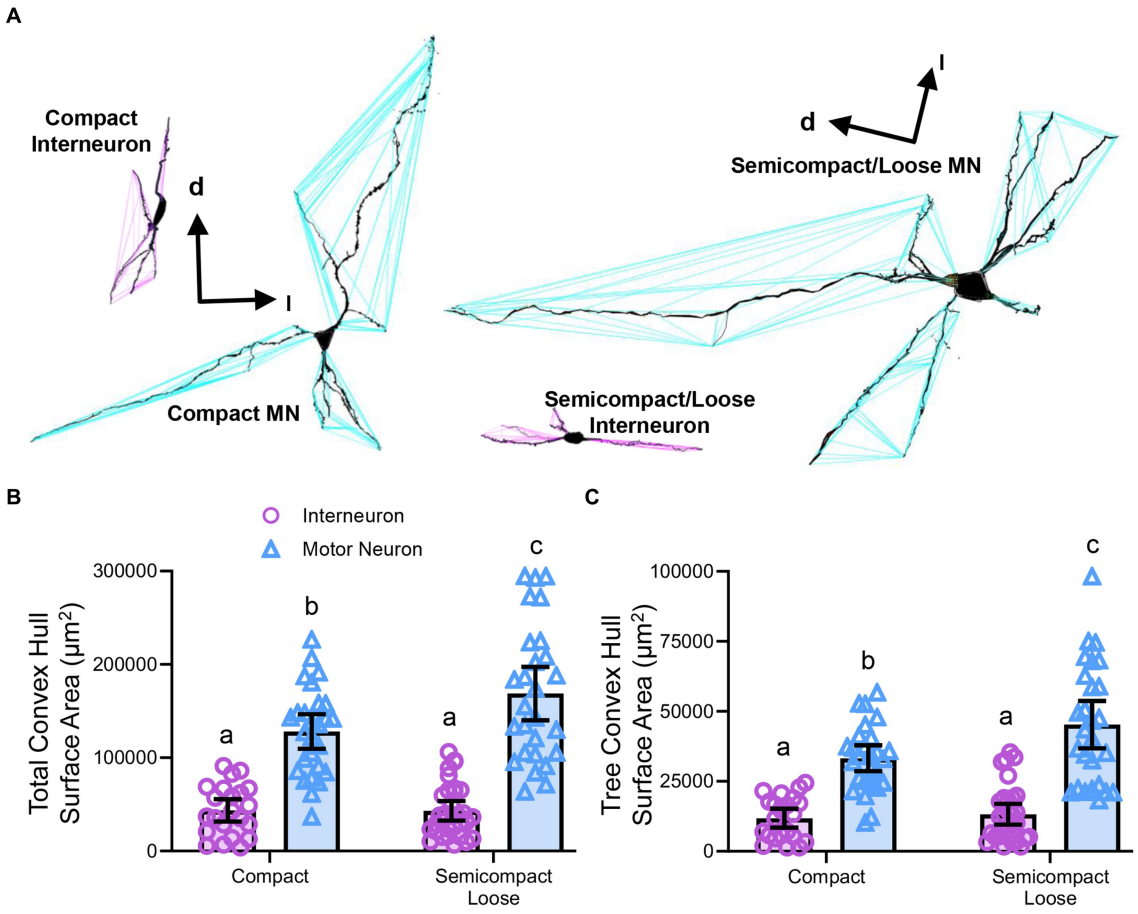

FIGURE 7
(A) 3D reconstruction of convex hulls (purple and blue polygons) of compact, semicompact/loose MNs and interneurons. **(B)** Plot shows smaller total dendritic tree convex hull surface areas (± 95% CI) in nucleus ambiguus interneurons compared to MNs, with semicompact/loose formation MN larger than compact formation MNs. **(C)** Plot shows smaller mean tree convex hull surface areas (± 95% CI) in nucleus ambiguus interneurons compared to MNs, with semicompact/loose formation MN larger than compact formation MNs. All analyses two-way ANOVAs with Bonferroni post-tests, with different letters denoting statistical differences between groups (i.e., $p < 0.05$). Dorsal (d) and lateral (l) are also indicated on the images.

the receptive fields of neurons within the nucleus ambiguus held to an identical outline, with convex hull surface areas extremely large in semicompact/loose formation MNs, large in compact formation MNs, and smallest in the interneurons. Moreover, our quantitative data are consistent with qualitative data in transverse brainstem slices of adult Sprague Dawley rats labelled with neurobiotin (Sun et al., 1995), where dendritic restrictions within the compact formation MNs were noted, compared to the more elaborate projections of laryngeal MNs within the semicompact formation.

In the present study, we did not examine the activities of the individual neurons, nor did we examine circuit activation and motor or cardiorespiratory responses. However, an abundance of prior retrograde tracing studies provides us with a reasonable idea of the normal physiological role of each neural population. These studies provide some clues as to why the morphologies of the MNs differ across regions within the nucleus ambiguus. As aforementioned, the MNs within the compact formation innervate the oesophagus (Holstege et al., 1983; Fryscak et al., 1984; Bieger and Hopkins, 1987; Altschuler et al., 1991), whilst the more caudal nucleus ambiguus MNs of the semicompact and loose formations innervate the palate and larynx (Hinrichsen and Ryan, 1981; Holstege et al., 1983; Flint et al., 1991; Hayakawa et al., 1996; Basken et al., 2012). Despite eschewing retrograde labelling, being largely incompatible with our Golgi approach, we used these extensive prior characterisations, the first-rate transverse-orientation rat brain atlas (Paxinos and Watson, 2014), and our cross-matching of histology in the Fischer 344 rat (this study). We therefore suggest that anatomical variability does not affect our study to a greater extent than the widely appreciated intermingling of neurons (particularly the ventrolateral respiratory group) within the semicompact/loose formations previously identified (Ellenberger and Feldman, 1990b; Sun et al., 1995). Although the nucleus ambiguus MN dendrites are reported to project in a longitudinal (parasagittal) manner (Bieger and Hopkins, 1987; Altschuler et al., 1991; Kruszewska et al., 1994; Hayakawa et al., 1996), two of these papers illustrate large transverse projections (Bieger and Hopkins, 1987; Altschuler et al., 1991), and one paper shows non-compact formation neuron, consistent with a semicompact/loose MN having extensive dorso-ventral projections (consistent with being oriented in the transverse plane) (Kruszewska et al., 1994). In addition, a prior study using intracellular labelling showed extensive arbourisation of nucleus ambiguus MNs in the transverse plane (Sun et al., 1995). Thus, given the advantages of anatomic orientation provided by transverse

sectioning (Figure 1), we proceeded with this approach—although our neuronal arbourisation quantifications may be an underestimate, particularly of total arbours as some trees of the compact formation MNs may have been obscured in the z-axis. Our final major limitation is the shrinkage of brainstem sections during processing (Kruszewska et al., 1994), which may hinder the classification of MNs, although this likely puts MNs in the interneuron category, due to reductions in size below the 30-μm-diameter MN threshold (Bieger and Hopkins, 1987; Altschuler et al., 1991; Hayakawa et al., 1996; Fogarty et al., 2018; Fogarty, 2023). Thus, our interneuron groups within the nucleus ambiguus dendritic assessments may include some of the smaller MNs. Indeed, these interneurons may be parasympathetic neurons, visceral and branchial efferents, gamma MNs, or shrunken small alpha MNs (Kalia and Mesulam, 1980; Hinrichsen and Ryan, 1981; Stuesse and Fish, 1984; Portillo and Pasaro, 1988a). Despite gamma MNs being important in other MN pools, it is unlikely that the smaller neurons in the population within the nucleus ambiguus contain gamma MNs as proprioception and muscle spindles are not readily identified in rat laryngeal muscles (Andrew, 1954, 1955, 1956a). So more correctly, the interneurons may be considered putative interneurons or non-MNs.

In the MNs of the compact formation, there is an overall need to coordinate oesophageal functions with ventilation. The close proximity of the compact region MNs and the relative restriction of their length and convex hull surface areas compared to semicompact/loose MNs is consistent with the necessity for synchronous activation of the cervical oesophagus and coordinated propagation in the thoracic and abdominal regions of the oesophagus (Altschuler et al., 1991; Kruszewska et al., 1994). The lack of extensive dendritic lengths at eighth and beyond branch orders is also consistent with this premise. This oesophageal activation in swallow is likely highly stereotyped in action [i.e., a reflex binary, initiated synchronously by distension or by the initiation of the swallow pattern (Andrew, 1956b; Meyer and Castell, 1982; Paterson, 1999; Broussard and Altschuler, 2000)], similar to the laryngeal functions in ventilation and swallow (Andrew, 1955; Fregosi and Ludlow, 2014; Huff et al., 2022; Pitts and Iceman, 2023). By contrast, laryngeal muscles operate over a wider range of behaviours (notably changes in pitch during vocalisation) (Wetzel et al., 1980; Bartlett and Knuth, 1984; Jurgens, 2009; Riede et al., 2020) and emotional states (Geyer et al., 1978; Geyer and Barfield, 1978; McIntosh et al., 1978; Barfield et al., 1979; Vanderhorst et al., 2000; Holstege, 2014), particularly in humans (Levin, 2006; Pisanski et al., 2022). Synchronous activation of MNs and their innervated muscle can be facilitated via: (i) gap junctions, which are not prevalent in oesophageal nucleus ambiguus MNs (Kruszewska et al., 1994); (ii) homogeneous high intrinsic excitability (i.e., less dendritic length/surface area leading to reduced neural capacitance), evident in findings of reduced dendritic surface areas and narrower ranges dendritic surface area in compact, compared to semicompact/loose MNs; and (iii) constrained dendritic projections, integrating inputs from fewer brainstem areas, evident in the reduced Sholl and dendritic convex hull surface areas of compact, compared to semicompact/loose MNs.

What remains evolutionarily peculiar is the observation that these oesophageal-innervating MNs are rostral to both pharyngeal MNs and the disparate brainstem swallow centres within the nucleus of the solitary tract and the dorsal and ventral swallow groups (Holstege et al., 1983; Kessler and Jean, 1985a,b; Zheng et al., 1997; Jean, 2001; Huff et al., 2022; Pitts and Iceman, 2023). Second, these neurons are activated last in the swallow phase—first oral, then pharyngeal, then oesophageal (Pitts and Iceman, 2023). Oesophageal activity seems impervious to unilateral dysfunction, due to a bilateral spread of innervated fibres within the oesophagus (Gruber, 1978). Moreover, in these rats, biochemical analysis of fibres is consistent with type IIa fibres, relatively resilient to age-associated weakness and denervation (Fogarty et al., 2019a, 2020a; Brown et al., 2021a; Sieck et al., 2023). Thus, the oesophageal functions and phase of swallow may be less vulnerable to perturbations of age and degeneration than those involved in the pharyngeal and oral phases. In particular, the resilience of compact formation nucleus ambiguus is evident in aged mice, where ~20% death of compact formation retrofacial nucleus ambiguus MNs compared to an overall loss of ~35% (Sturrock, 1990). In brainstem and spinal MNs of rats and humans, there are known motor unit type-dependent differences in vulnerability, with slow and fatigue-resistant MNs resilient and fatigueable MNs prone to death in old age (Hashizume et al., 1988; Kanda and Hashizume, 1998; Fogarty et al., 2018; Fogarty, 2023) and neurodegenerative conditions (Kiernan and Hudson, 1991; Pun et al., 2006; Dukkipati et al., 2018). Type-dependent differences in dendritic arbours, with larger MNs having larger arbours MNs (Cullheim et al., 1987; Ma and Vacca-Galloway, 1991; Leroy et al., 2014; Fogarty et al., 2019b, 2020b) and synaptic inputs, larger MNs having more excitatory inputs (Kellerth et al., 1979; Brannstrom, 1993) exist in MNs and may underpin differential susceptibility to degeneration and death (Ahmed et al., 2016; Fogarty, 2018; Kiernan et al., 2019). Our current observation of relatively restricted dendritic arbour size and previous quantifications of less synaptic inputs compared to pharyngeal MNs (Hayakawa et al., 1996) is consistent with a propensity of this region to harbour MNs comprising fatigue-resistant (slow or fast) motor units. It remains to be determined whether compact formation MNs and their dendritic arbours are conserved with age and neurodegeneration in the rat. We would expect that in old age, compact formation MNs would be spared in number and degenerative phenotype.

The MNs of the semicompact/loose formations, innervating the palate and laryngeal muscles, are activated during vocalisation and the oral and pharyngeal phases of swallow (Wetzel et al., 1980; Holstege et al., 1983; Holstege, 1989; Vanderhorst et al., 2000; Jurgens, 2009). Indeed, interactions between emotional processing centres of the brainstem and the muscles of speech/vocalisation are becoming increasingly studied (Vanderhorst et al., 2000; Holstege, 2014; Subramanian et al., 2018, 2021). Similarly to oesophageal MNs, these MNs must coordinate their activation with the control of breathing as well as vomiting, cough, and a host of other behaviours (Kessler and Jean, 1985b; Car and Amri, 1987; Tomomune and Takata, 1988; Amri et al., 1991; Nishino and Hiraga, 1991; Dick et al., 1993; Umezaki et al., 1998; Jean, 2001; Sawczuk and Mosier, 2001; Roda et al., 2002; Pitts et al., 2012; Fregosi and Ludlow, 2014; Huff et al., 2022). Thus, compared to oesophageal MNs, palate and laryngeal MNs must integrate their activities across a wider range of behavioural states. The exaggerated length and convex hull surface area to provide the substrate for synaptic inputs from diverse sources is evident in the current study and is consistent with synaptic inputs quantified by electron microscopy and qualitative assessments in Sprague Dawley rats (Sun et al., 1995; Hayakawa et al., 1996). The larger range of dendritic sizes is consistent with a more diverse motor unit population, confirmed by the mixed myosin heavy chain expressions confirming type I, IIa, IIx, IIb, and mixtures of IIx and IIb with extraocular fibres in cricothyroid, cricoarytenoid, and thyroarytenoid muscles (Rhee et al., 2004). Thus, within the semicompact/loose formations of the

nucleus ambiguus there resides age- and neurodegeneration-vulnerable and resilient MNs innervating the larynx, similar to other mixed motor unit population motor pools (Fogarty et al., 2018; Fogarty, 2023; Fogarty and Sieck, 2023). This is borne out in observations of dysphagia and dysphonia in the elderly, in Alzheimer's disease and amyotrophic lateral sclerosis sufferers (Turley and Cohen, 2009; Humbert et al., 2010; Christmas and Rogus-Pulia, 2019; Garand et al., 2022), alongside rodent studies of aged Fischer 344–Brown Norway crosses (Basken et al., 2012; Krekeler et al., 2020). In particular, the study by Basken showed a specific loss of retrogradely labelled laryngeal MNs (Basken et al., 2012), although it remains unconfirmed whether these findings hold in Fischer 344 rats. It is likely that vulnerable MNs in this population will exhibit distal dendritic pathology consistent with degeneration.

Conclusion

In conclusion, this study presents the first comprehensive quantitative evaluation of the dendritic morphologies of MNs and non-MNs within the compact, semicompact, and loose formations of the nucleus ambiguus. Our findings in MNs are consistent with motor unit type-specific differences between the different regions. Our findings are also consistent with differences in the number of different behaviours each motor pool must coordinate its activities with. These findings provide a solid basis with which to assess various developmental, ageing, and disease states.

Data availability statement

The original contributions presented in the study are included in the article/supplementary material, further inquiries can be directed to the corresponding author.

Ethics statement

The animal study was approved by Mayo Clinic Institute Animal Care and Use Committee (IACUC approval #A57714). The study was conducted in accordance with the local legislation and institutional requirements.

Author contributions

MF: Conceptualization, Data curation, Formal analysis, Funding acquisition, Investigation, Methodology, Project administration, Resources, Software, Supervision, Validation, Visualization, Writing – original draft, Writing – review & editing.

Funding

The author(s) declare financial support was received for the research, authorship, and/or publication of this article. Funding for this study was provided by the NIH R56-HL166204.

Acknowledgments

We would like to thank Yun-Hua Fang and Becky Macken for aiding the completion of this project.

Conflict of interest

The author declares that the research was conducted in the absence of any commercial or financial relationships that could be construed as a potential conflict of interest.

Publisher's note

References

Ahmed, R. M., Devenney, E. M., Irish, M., Ittner, A., Naismith, S., Ittner, L. M., et al. (2016). Neuronal network disintegration: common pathways linking neurodegenerative diseases. *J. Neurol. Neurosurg. Psychiatry* 87, 1234–1241. doi: 10.1136/jnnp-2014-308350

Altschuler, S. M., Bao, X. M., and Miselis, R. R. (1991). Dendritic architecture of nucleus ambiguus motoneurons projecting to the upper alimentary tract in the rat. *J. Comp. Neurol.* 309, 402–414. doi: 10.1002/cne.903090309

Amri, M., Lamkadem, M., and Car, A. (1991). Effects of lingual nerve and chewing cortex stimulation upon activity of the swallowing neurons located in the region of the hypoglossal motor nucleus. *Brain Res.* 548, 149–155. doi: 10.1016/0006-8993(91)91116-I

Andrew, B. L. (1954). Proprioception at the joint of the epiglottis of the rat. *J. Physiol.* 126, 507–523. doi: 10.1113/jphysiol.1954.sp005225

Andrew, B. L. (1955). The respiratory displacement of the larynx: a study of the innervation of accessory respiratory muscles. *J. Physiol.* 130, 474–487. doi: 10.1113/jphysiol.1955.sp005421

Andrew, B. L. (1956a). A functional analysis of the myelinated fibres of the superior laryngeal nerve of the rat. *J. Physiol.* 133, 420–432. doi: 10.1113/jphysiol.1956.sp005597

Andrew, B. L. (1956b). The nervous control of the cervical oesophagus of the rat during swallowing. *J. Physiol.* 134, 729–740. doi: 10.1113/jphysiol.1956.sp005679

Barfield, R. J., Auerbach, P., Geyer, L. A., and Mcintosh, T. K. (1979). Ultrasonic vocalizations in rat sexual-behavior. *Am. Zool.* 19, 469–480. doi: 10.1093/icb/19.2.469

Bartlett, D. J., and Knuth, S. L. (1984). Human vocal cord movements during voluntary hyperventilation. *Respir. Physiol.* 58, 289–294. doi: 10.1016/0034-5687(84)90005-7

Basken, J. N., Connor, N. P., and Ciucci, M. R. (2012). Effect of aging on ultrasonic vocalizations and laryngeal sensorimotor neurons in rats. *Exp. Brain Res.* 219, 351–361. doi: 10.1007/s00221-012-3096-6

Bieger, D., and Hopkins, D. A. (1987). Viscerotopic representation of the upper alimentary tract in the medulla oblongata in the rat: the nucleus ambiguus. *J. Comp. Neurol.* 262, 546–562. doi: 10.1002/cne.902620408

Bird, A. D., and Cuntz, H. (2019). Dissecting Sholl analysis into its functional components. *Cell Rep.* 27:e3085, 3081–3096.e5. doi: 10.1016/j.celrep.2019.04.097

Bolser, D. C., Pitts, T. E., Davenport, P. W., and Morris, K. F. (2015). Role of the dorsal medulla in the neurogenesis of airway protection. *Pulm. Pharmacol. Ther.* 35, 105–110. doi: 10.1016/j.pupt.2015.10.012

Brandenburg, J. E., Fogarty, M. J., Brown, A. D., and Sieck, G. C. (2020). Phrenic motor neuron loss in an animal model of early onset hypertonia. *J. Neurophysiol.* 123, 1682–1690. doi: 10.1152/jn.00026.2020

Brandenburg, J. E., Gransee, H. M., Fogarty, M. J., and Sieck, G. C. (2018). Differences in lumbar motor neuron pruning in an animal model of early onset spasticity. *J. Neurophysiol.* 120, 601–609. doi: 10.1152/jn.00186.2018

Brannstrom, T. (1993). Quantitative synaptology of functionally different types of cat medial gastrocnemius alpha-motoneurons. *J. Comp. Neurol.* 330, 439–454. doi: 10.1002/cne.903300311

Broussard, D. L., and Altschuler, S. M. (2000). Central integration of swallow and airway-protective reflexes. *Am. J. Med.* 108, 62–67. doi: 10.1016/S0002-9343(99)00340-X

Brown, A. D., Davis, L. A., Fogarty, M. J., and Sieck, G. C. (2021a). Mitochondrial fragmentation and dysfunction in type IIx/IIb diaphragm muscle fibers in 24-month old Fischer 344 rats. *Front. Physiol.* 12:727585. doi: 10.3389/fphys.2021.727585

Brown, A. D., Fogarty, M. J., and Sieck, G. C. (2021b). Mitochondrial morphology and function varies across diaphragm muscle fiber types. *Respir. Physiol. Neurobiol.* 295:103780. doi: 10.1016/j.resp.2021.103780

Burke, R. E., Levine, D. N., Tsairis, P., and Zajac, F. E. (1973). Physiological types and histochemical profiles in motor units of the cat gastrocnemius. *J. Physiol.* 234, 723–748. doi: 10.1113/jphysiol.1973.sp010369

Car, A., and Amri, M. (1987). Activity of neurons located in the region of the hypoglossal motor nucleus during swallowing in sheep. *Exp. Brain Res.* 69, 175–182. doi: 10.1007/BF00247040

Christmas, C., and Rogus-Pulia, N. (2019). Swallowing disorders in the older population. *J. Am. Geriatr. Soc.* 67, 2643–2649. doi: 10.1111/jgs.16137

Coverdell, T. C., Abraham-Fan, R. J., Wu, C., Abbott, S. B. G., and Campbell, J. N. (2022). Genetic encoding of an esophageal motor circuit. *Cell Rep.* 39:110962. doi: 10.1016/j.celrep.2022.110962

Cullheim, S., Fleshman, J. W., Glenn, L. L., and Burke, R. E. (1987). Membrane area and dendritic structure in type-identified triceps surae alpha motoneurons. *J. Comp. Neurol.* 255, 68–81. doi: 10.1002/cne.902550106

Davis, P. J., and Nail, B. S. (1984). On the location and size of laryngeal motoneurons in the cat and rabbit. *J. Comp. Neurol.* 230, 13–32. doi: 10.1002/cne.902300103

Dick, T. E., Kong, F. J., and Berger, A. J. (1987). Correlation of recruitment order with axonal conduction velocity for supraspinally driven diaphragmatic motor units. *J. Neurophysiol.* 57, 245–259. doi: 10.1152/jn.1987.57.1.245

Dick, T. E., Oku, Y., Romaniuk, J. R., and Cherniack, N. S. (1993). Interaction between central pattern generators for breathing and swallowing in the cat. *J. Physiol.* 465, 715–730. doi: 10.1113/jphysiol.1993.sp019702

Dobbins, E. G., and Feldman, J. L. (1995). Differential innervation of protruder and retractor muscles of the tongue in rat. *J. Comp. Neurol.* 357, 376–394. doi: 10.1002/cne.903570305

Dukkipati, S. S., Garrett, T. L., and Elbasiouny, S. M. (2018). The vulnerability of spinal motoneurons and soma size plasticity in a mouse model of amyotrophic lateral sclerosis. *J. Physiol.* 596, 1723–1745. doi: 10.1113/JP275498

Ellenberger, H. H., and Feldman, J. L. (1990a). Brainstem connections of the rostral ventral respiratory group of the rat. *Brain Res.* 513, 35–42. doi: 10.1016/0006-8993(90)91086-V

Ellenberger, H. H., and Feldman, J. L. (1990b). Subnuclear organization of the lateral tegmental field of the rat. 1: nucleus ambiguus and ventral respiratory group. *J. Comp. Neurol.* 294, 202–211. doi: 10.1002/cne.902940205

Flint, P. W., Downs, D. H., and Coltrera, M. D. (1991). Laryngeal synkinesis following reinnervation in the rat. Neuroanatomic and physiologic study using retrograde fluorescent tracers and electromyography. *Ann. Otol. Rhinol. Laryngol.* 100, 797–806. doi: 10.1177/000348949110001003

Fogarty, M. J. (2018). Driven to decay: excitability and synaptic abnormalities in amyotrophic lateral sclerosis. *Brain Res. Bull.* 140, 318–333. doi: 10.1016/j.brainresbull.2018.05.023

Fogarty, M. J. (2023). Loss of larger hypoglossal motor neurons in aged Fischer 344 rats. *Respir. Physiol. Neurobiol.* 314:104092. doi: 10.1016/j.resp.2023.104092

Fogarty, M. J., Kanjhan, R., Bellingham, M. C., and Noakes, P. G. (2016a). Glycinergic neurotransmission: a potent regulator of embryonic motor neuron dendritic morphology and synaptic plasticity. *J. Neurosci.* 36, 80–87. doi: 10.1523/JNEUROSCI.1576-15.2016

Fogarty, M. J., Kanjhan, R., Yanagawa, Y., Noakes, P. G., and Bellingham, M. C. (2017a). Alterations in hypoglossal motor neurons due to GAD67 and VGAT deficiency in mice. *Exp. Neurol.* 289, 117–127. doi: 10.1016/j.expneurol.2016.12.004

Fogarty, M. J., Mantilla, C. B., and Sieck, G. C. (2019a). Impact of sarcopenia on diaphragm muscle fatigue. *Exp. Physiol.* 104, 1090–1099. doi: 10.1113/EP087558

Fogarty, M. J., Marin Mathieu, N., Mantilla, C. B., and Sieck, G. C. (2020a). Aging reduces succinate dehydrogenase activity in rat type IIx/IIb diaphragm muscle fibers. *J. Appl. Physiol.* 128, 70–77. doi: 10.1152/japplphysiol.00644.2019

Fogarty, M. J., Mu, E. W. H., Lavidis, N. A., Noakes, P. G., and Bellingham, M. C. (2017b). Motor areas show altered dendritic structure in an amyotrophic lateral sclerosis mouse model. *Front. Neurosci.* 11:609. doi: 10.3389/fnins.2017.00609

Fogarty, M. J., Mu, E. W., Lavidis, N. A., Noakes, P. G., and Bellingham, M. C. (2019b). Size-dependent vulnerability of lumbar motor neuron dendritic degeneration in SOD1G93A mice. *Anat Rec (Hoboken).* 303:1455–1471. doi: 10.1002/ar.24255

Fogarty, M. J., Mu, E. W. H., Lavidis, N. A., Noakes, P. G., and Bellingham, M. C. (2020b). Size-dependent dendritic maladaptations of hypoglossal motor neurons in SOD1(G93A) mice. *Anat Rec (Hoboken).* 303, 1455–1471. doi: 10.1002/ar.24255

Fogarty, M. J., Mu, E. W., Noakes, P. G., Lavidis, N. A., and Bellingham, M. C. (2016b). Marked changes in dendritic structure and spine density precede significant neuronal death in vulnerable cortical pyramidal neuron populations in the SOD1(G93A) mouse model of amyotrophic lateral sclerosis. *Acta Neuropathol. Commun.* 4:77. doi: 10.1186/s40478-016-0347-y

Fogarty, M. J., Omar, T. S., Zhan, W. Z., Mantilla, C. B., and Sieck, G. C. (2018). Phrenic motor neuron loss in aged rats. *J. Neurophysiol.* 119, 1852–1862. doi: 10.1152/jn.00868.2017

Fogarty, M. J., and Sieck, G. C. (2019). Evolution and functional differentiation of the diaphragm muscle of mammals. *Compr. Physiol.* 9, 715–766. doi: 10.1002/cphy.c180012

Fogarty, M. J., and Sieck, G. C. (2021). Tongue muscle contractile, fatigue, and fiber type properties in rats. *J. Appl. Physiol.* 131, 1043–1055. doi: 10.1152/japplphysiol.00329.2021

Fogarty, M. J., and Sieck, G. C. (2023). Aging affects the number and morphological heterogeneity of rat phrenic motor neurons and phrenic motor axons. *Physiol. Rep.* 11:e15587. doi: 10.14814/phy2.15587

Fogarty, M. J., Smallcombe, K. L., Yanagawa, Y., Obata, K., Bellingham, M. C., and Noakes, P. G. (2013). Genetic deficiency of GABA differentially regulates respiratory and non-respiratory motor neuron development. *PLoS One* 8:e56257. doi: 10.1371/journal.pone.0056257

Fogarty, M. J., Yanagawa, Y., Obata, K., Bellingham, M. C., and Noakes, P. G. (2015). Genetic absence of the vesicular inhibitory amino acid transporter differentially regulates respiratory and locomotor motor neuron development. *Brain Struct. Funct.* 220, 525–540. doi: 10.1007/s00429-013-0673-9

Fregosi, R. F., and Ludlow, C. L. (2014). Activation of upper airway muscles during breathing and swallowing. *J. Appl. Physiol.* 116, 291–301. doi: 10.1152/japplphysiol.00670.2013

Fryscak, T., Zenker, W., and Kantner, D. (1984). Afferent and efferent innervation of the rat esophagus. A tracing study with horseradish peroxidase and nuclear yellow. *Anat Embryol (Berl)* 170, 63–70. doi: 10.1007/BF00319459

Garand, K. L. F., Bhutada, A. M., Hopkins-Rossabi, T., Mulekar, M. S., and Carnaby, G. (2022). Pilot study of respiratory-swallow coordination in amyotrophic lateral sclerosis. *J. Speech Lang. Hear. Res.* 65, 2815–2828. doi: 10.1044/2022_JSLHR-21-00619

Geyer, L. A., and Barfield, R. J. (1978). Influence of gonadal hormones and sexual behavior on ultrasonic vocalization in rats: I. Treatment of females. *J. Comp. Physiol. Psychol.* 92, 438–446. doi: 10.1037/h0077480

Geyer, L. A., Barfield, R. J., and Mcintosh, T. K. (1978). Influence of gonadal hormones and sexual behavior on ultrasonic vocalization in rats: II. Treatment of males. *J. Comp. Physiol. Psychol.* 92, 447–456. doi: 10.1037/h0077487

Glaser, E. M., and Van Der Loos, H. (1981). Analysis of thick brain sections by obverse-reverse computer microscopy: application of a new, high clarity Golgi-Nissl stain. *J. Neurosci. Methods* 4, 117–125. doi: 10.1016/0165-0270(81)90045-5

Gruber, H. (1978). Motor innervation of striated oesophageal muscle. Part 2. Characteristics of the oesophagomotor fibres in the rat studied by implanting the vagus nerve into a skeletal muscle. *J. Neurol. Sci.* 36, 171–186. doi: 10.1016/0022-510X(78)90081-3

Hashizume, K., Kanda, K., and Burke, R. E. (1988). Medial gastrocnemius motor nucleus in the rat: age-related changes in the number and size of motoneurons. *J. Comp. Neurol.* 269, 425–430. doi: 10.1002/cne.902690309

Hayakawa, T., Yajima, Y., and Zyo, K. (1996). Ultrastructural characterization of pharyngeal and esophageal motoneurons in the nucleus ambiguus of the rat. *J. Comp. Neurol.* 370, 135–146. doi: 10.1002/(SICI)1096-9861(19960624)370:2<135::AID-CNE1>3.0.CO;2-3

Heckman, C. J., and Enoka, R. M. (2012). Motor unit. *Compr. Physiol.* 2, 2629–2682. doi: 10.1002/cphy.c100087

Hernandez-Morato, I., Pascual-Font, A., Ramirez, C., Matarranz-Echeverria, J., Mchanwell, S., Vazquez, T., et al. (2013). Somatotopy of the neurons innervating the cricothyroid, posterior cricoarytenoid, and thyroarytenoid muscles of the rat's larynx. *Anat Rec (Hoboken)* 296, 470–479. doi: 10.1002/ar.22643

Hinrichsen, C., and Dulhunty, A. (1982). The contractile properties, histochemistry, ultrastructure and electrophysiology of the cricothyroid and posterior cricoarytenoid muscles in the rat. *J. Muscle Res. Cell Motil.* 3, 169–190. doi: 10.1007/BF00711941

Hinrichsen, C. F., and Ryan, A. T. (1981). Localization of laryngeal motoneurons in the rat: morphologic evidence for dual innervation? *Exp. Neurol.* 74, 341–355. doi: 10.1016/0014-4886(81)90174-6

Holstege, G. (1989). Anatomical study of the final common pathway for vocalization in the cat. *J. Comp. Neurol.* 284, 242–252. doi: 10.1002/cne.902840208

Holstege, G. (2014). The periaqueductal gray controls brainstem emotional motor systems including respiration. *Prog. Brain Res.* 209, 379–405. doi: 10.1016/B978-0-444-63274-6.00020-5

Holstege, G., Graveland, G., Bijker-Biemond, C., and Schuddeboom, I. (1983). Location of motoneurons innervating soft palate, pharynx and upper esophagus. Anatomical evidence for a possible swallowing center in the pontine reticular formation. An HRP and autoradiographical tracing study. *Brain Behav. Evol.* 23, 47–62. doi: 10.1159/000121488

Huff, A., Karlen-Amarante, M., Pitts, T., and Ramirez, J. M. (2022). Optogenetic stimulation of pre-Botzinger complex reveals novel circuit interactions in swallowing-breathing coordination. *Proc. Natl. Acad. Sci. USA* 119:e2121095119. doi: 10.1073/pnas.2121095119

Humbert, I. A., Mclaren, D. G., Kosmatka, K., Fitzgerald, M., Johnson, S., Porcaro, E., et al. (2010). Early deficits in cortical control of swallowing in Alzheimer's disease. *J. Alzheimers Dis.* 19, 1185–1197. doi: 10.3233/JAD-2010-1316

Jacob, J. M. (1998). Lumbar motor neuron size and number is affected by age in male F344 rats. *Mech. Ageing Dev.* 106, 205–216. doi: 10.1016/S0047-6374(98)00117-1

Jean, A. (2001). Brain stem control of swallowing: neuronal network and cellular mechanisms. *Physiol. Rev.* 81, 929–969. doi: 10.1152/physrev.2001.81.2.929

Johnson, I. P., and Duberley, R. M. (1998). Motoneuron survival and expression of neuropeptides and neurotrophic factor receptors following axotomy in adult and ageing rats. *Neuroscience* 84, 141–150. doi: 10.1016/S0306-4522(97)00500-9

Jurgens, U. (2009). The neural control of vocalization in mammals: a review. *J. Voice* 23, 1–10. doi: 10.1016/j.jvoice.2007.07.005

Kalia, M., and Mesulam, M. M. (1980). Brain stem projections of sensory and motor components of the vagus complex in the cat: II. Laryngeal, tracheobronchial, pulmonary, cardiac, and gastrointestinal branches. *J. Comp. Neurol.* 193, 467–508. doi: 10.1002/cne.901930211

Kanda, K., and Hashizume, K. (1998). Effects of long-term physical exercise on age-related changes of spinal motoneurons and peripheral nerves in rats. *Neurosci. Res.* 31, 69–75. doi: 10.1016/S0168-0102(98)00026-1

Kanjhan, R., Fogarty, M. J., Noakes, P. G., and Bellingham, M. C. (2016). Developmental changes in the morphology of mouse hypoglossal motor neurons. *Brain Struct. Funct.* 221, 3755–3786. doi: 10.1007/s00429-015-1130-8

Kecskes, S., Koszeghy, A., Szucs, G., Rusznak, Z., Matesz, C., and Birinyi, A. (2013). Three-dimensional reconstruction and quantitative morphometric analysis of pyramidal and giant neurons of the rat dorsal cochlear nucleus. *Brain Struct. Funct.* 218, 1279–1292. doi: 10.1007/s00429-012-0457-7

Kellerth, J. O., Berthold, C. H., and Conradi, S. (1979). Electron microscopic studies of serially sectioned cat spinal alpha-motoneurons. *J. Comp. Neurol.* 184, 755–767. doi: 10.1002/cne.901840408

Kessler, J. P., and Jean, A. (1985a). Identification of the medullary swallowing regions in the rat. *Exp. Brain Res.* 57, 256–263

Kessler, J. P., and Jean, A. (1985b). Inhibition of the swallowing reflex by local application of serotonergic agents into the nucleus of the solitary tract. *Eur. J. Pharmacol.* 118, 77–85. doi: 10.1016/0014-2999(85)90665-X

Kiernan, J. A., and Hudson, A. J. (1991). Changes in sizes of cortical and lower motor neurons in amyotrophic lateral sclerosis. *Brain* 114, 843–853. doi: 10.1093/brain/114.2.843

Kiernan, M. C., Ziemann, U., and Eisen, A. (2019). Amyotrophic lateral sclerosis: origins traced to impaired balance between neural excitation and inhibition in the neonatal period. *Muscle Nerve* 60, 232–235. doi: 10.1002/mus.26617

Klenowski, P. M., Fogarty, M. J., Belmer, A., Noakes, P. G., Bellingham, M. C., and Bartlett, S. E. (2015). Structural and functional characterization of dendritic arbors and GABAergic synaptic inputs on interneurons and principal cells in the rat basolateral amygdala. *J. Neurophysiol.* 114, 942–957. doi: 10.1152/jn.00824.2014

Klenowski, P. M., Shariff, M. R., Belmer, A., Fogarty, M. J., Mu, E. W., Bellingham, M. C., et al. (2016). Prolonged consumption of sucrose in a binge-like manner, alters the morphology of medium spiny neurons in the nucleus Accumbens Shell. *Front. Behav. Neurosci.* 10:54. doi: 10.3389/fnbeh.2016.00054

Krekeler, B. N., Weycker, J. M., and Connor, N. P. (2020). Effects of tongue exercise frequency on tongue muscle biology and swallowing physiology in a rat model. *Dysphagia* 35, 918–934. doi: 10.1007/s00455-020-10105-2

Kruszewska, B., Lipski, J., and Kanjhan, R. (1994). An electrophysiological and morphological study of esophageal motoneurons in rats. *Am. J. Phys.* 266, R622–R632. doi: 10.1152/ajpregu.1994.266.2.R622

Kubota, Y., Karube, F., Nomura, M., Gulledge, A. T., Mochizuki, A., Schertel, A., et al. (2011). Conserved properties of dendritic trees in four cortical interneuron subtypes. *Sci. Rep.* 1:89. doi: 10.1038/srep00089

Lance-Jones, C. (1982). Motoneuron cell death in the developing lumbar spinal cord of the mouse. *Brain Res.* 256, 473–479. doi: 10.1016/0165-3806(82)90192-4

Lawn, A. M. (1966). The localization, in the nucleus ambiguus of the rabbit, of the cells of origin of motor nerve fibers in the glossopharyngeal nerve and various branches of the vagus nerve by means of retrograde degeneration. *J. Comp. Neurol.* 127, 293–305. doi: 10.1002/cne.901270210

Leroy, F., Lamotte D'incamps, B., Imhoff-Manuel, R. D., and Zytnicki, D. (2014). Early intrinsic hyperexcitability does not contribute to motoneuron degeneration in amyotrophic lateral sclerosis. *eLife* 3:e04046. doi: 10.7554/eLife.04046

Levin, R. J. (2006). Vocalised sounds and human sex. *Sex. Relatsh. Ther.* 21, 99–107. doi: 10.1080/14681990500438014

Ma, W. Y., and Vacca-Galloway, L. L. (1991). Reduced branching and length of dendrites detected in cervical spinal cord motoneurons of wobbler mouse, a model for inherited motoneuron disease. *J. Comp. Neurol.* 311, 210–222. doi: 10.1002/cne.903110204

Malmierca, M. S., Seip, K. L., and Osen, K. K. (1995). Morphological classification and identification of neurons in the inferior colliculus: a multivariate analysis. *Anat Embryol (Berl)* 191, 343–350. doi: 10.1007/BF00534687

Mantilla, C. B., Zhan, W. Z., and Sieck, G. C. (2009). Retrograde labeling of phrenic motoneurons by intrapleural injection. *J. Neurosci. Methods* 182, 244–249. doi: 10.1016/j.jneumeth.2009.06.016

Marino, J. P., and Johns, M. M. (2014). The epidemiology of dysphonia in the aging population. *Curr. Opin. Otolaryngol. Head Neck Surg.* 22, 455–459. doi: 10.1097/MOO.0000000000000098

Marks, W. B., and Burke, R. E. (2007). Simulation of motoneuron morphology in three dimensions. II. Building complete neurons. *J Comp Neurol* 503, 701–716. doi: 10.1002/cne.21417

Mazzone, S. B., and Canning, B. J. (2013). Autonomic neural control of the airways. *Handb. Clin. Neurol.* 117, 215–228. doi: 10.1016/B978-0-444-53491-0.00018-3

Mcallen, R. M., and Spyer, K. M. (1978). Two types of vagal preganglionic motoneurones projecting to the heart and lungs. *J. Physiol.* 282, 353–364. doi: 10.1113/jphysiol.1978.sp012468

Mcgovern, A. E., and Mazzone, S. B. (2010). Characterization of the vagal motor neurons projecting to the Guinea pig airways and esophagus. *Front. Neurol.* 1:153. doi: 10.3389/fneur.2010.00153

Mcintosh, T. K., Barfield, R. J., and Geyer, L. A. (1978). Ultrasonic vocalisations facilitate sexual behaviour of female rats. *Nature* 272, 163–164. doi: 10.1038/272163a0

Meyer, G. W., and Castell, D. O. (1982). Physiology of the oesophagus. *Clin. Gastroenterol.* 11, 439–451. doi: 10.1016/S0300-5089(21)00539-3

Monnier, A., Alheid, G. F., and Mccrimmon, D. R. (2003). Defining ventral medullary respiratory compartments with a glutamate receptor agonist in the rat. *J. Physiol.* 548, 859–874. doi: 10.1113/jphysiol.2002.038141

Neuhuber, W. L., and Berthoud, H. R. (2022). Functional anatomy of the vagus system: how does the polyvagal theory comply? *Biol. Psychol.* 174:108425. doi: 10.1016/j.biopsycho.2022.108425

Nishino, T., and Hiraga, K. (1991). Coordination of swallowing and respiration in unconscious subjects. *J. Appl. Physiol.* 70, 988–993. doi: 10.1152/jappl.1991.70.3.988

Nosaka, S., Yamamoto, T., and Yasunaga, K. (1979). Localization of vagal cardioinhibitory preganglionic neurons with rat brain stem. *J. Comp. Neurol.* 186, 79–92. doi: 10.1002/cne.901860106

Odutola, A. B. (1976). Cell grouping and Golgi architecture of the hypoglossal nucleus of the rat. *Exp. Neurol.* 52, 356–371. doi: 10.1016/0014-4886(76)90211-9

Paterson, W. G. (1999). Alteration of swallowing and oesophageal peristalsis by different initiators of deglutition. *Neurogastroenterol. Motil.* 11, 63–67. doi: 10.1046/j.1365-2982.1999.00131.x

Paxinos, G. (1999). *Chemoarchitectonic Atlas of the Rat Brainstem*. San Diego: Academic Press.

Paxinos, G., and Watson, C. (2014). *Paxino's and Watson's the Rat Brain in Stereotaxic Coordinates*. Amsterdam; Boston: Elsevier/AP, Academic Press Is an Imprint of Elsevier.

Pisanski, K., Bryant, G. A., Cornec, C., Anikin, A., and Reby, D. (2022). Form follows function in human nonverbal vocalisations. *Ethol. Ecol. Evol.* 34, 303–321. doi: 10.1080/03949370.2022.2026482

Pitts, T., and Iceman, K. E. (2023). Deglutition and the regulation of the swallow motor pattern. *Physiology (Bethesda)* 38, 10–24. doi: 10.1152/physiol.00005.2021

Pitts, T., Morris, K., Lindsey, B., Davenport, P., Poliacek, I., and Bolser, D. (2012). Co-ordination of cough and swallow in vivo and in silico. *Exp. Physiol.* 97, 469–473. doi: 10.1113/expphysiol.2011.063362

Porter, J. T., Johnson, C. K., and Agmon, A. (2001). Diverse types of interneurons generate thalamus-evoked feedforward inhibition in the mouse barrel cortex. *J. Neurosci.* 21, 2699–2710. doi: 10.1523/JNEUROSCI.21-08-02699.2001

Portillo, F., and Pasaro, R. (1988a). Location of bulbospinal neurons and of laryngeal motoneurons within the nucleus ambiguus of the rat and cat by means of retrograde fluorescent labelling. *J. Anat.* 159, 11–18

Portillo, F., and Pasaro, R. (1988b). Location of motoneurons supplying the intrinsic laryngeal muscles of rats. Horseradish peroxidase and fluorescence double-labeling study. *Brain Behav. Evol.* 32, 220–225. doi: 10.1159/000116549

Pun, S., Santos, A. F., Saxena, S., Xu, L., and Caroni, P. (2006). Selective vulnerability and pruning of phasic motoneuron axons in motoneuron disease alleviated by CNTF. *Nat. Neurosci.* 9, 408–419. doi: 10.1038/nn1653

Rall, W. (1959). Branching dendritic trees and motoneuron membrane resistivity. *Exp. Neurol.* 1, 491–527. doi: 10.1016/0014-4886(59)90046-9

Rall, W. (1960). Membrane potential transients and membrane time constant of motoneurons. *Exp. Neurol.* 2, 503–532. doi: 10.1016/0014-4886(60)90029-7

Rall, W. (1977). "Core conductor theory and cable properties of neurons," in handbook of physiology: the nervous system, ed. E.R. *Kandel* 1977, 39–97.

Rhee, H. S., Lucas, C. A., and Hoh, J. F. (2004). Fiber types in rat laryngeal muscles and their transformations after denervation and reinnervation. *J. Histochem. Cytochem.* 52, 581–590. doi: 10.1177/002215540405200503

Riede, T., Schaefer, C., and Stein, A. (2020). Role of deep breaths in ultrasonic vocal production of Sprague-Dawley rats. *J. Neurophysiol.* 123, 966–979. doi: 10.1152/jn.00590.2019

Roda, F., Gestreau, C., and Bianchi, A. L. (2002). Discharge patterns of hypoglossal motoneurons during fictive breathing, coughing, and swallowing. *J. Neurophysiol.* 87, 1703–1711. doi: 10.1152/jn.00347.2001

Rojo, C., Leguey, I., Kastanauskaite, A., Bielza, C., Larranaga, P., Defelipe, J., et al. (2016). Laminar differences in dendritic structure of pyramidal neurons in the juvenile rat somatosensory cortex. *Cereb. Cortex* 26, 2811–2822. doi: 10.1093/cercor/bhv316

Sawczuk, A., and Mosier, K. M. (2001). Neural control of tongue movement with respect to respiration and swallowing. *Crit. Rev. Oral Biol. Med.* 12, 18–37. doi: 10.1177/10454411010120010101

Schneider, C. A., Rasband, W. S., and Eliceiri, K. W. (2012). NIH image to ImageJ: 25 years of image analysis. *Nat. Methods* 9, 671–675. doi: 10.1038/nmeth.2089

Sholl, D. A. (1953). Dendritic organization in the neurons of the visual and motor cortices of the cat. *J. Anat.* 87, 387–406.

Sieck, G. C., Hernandez-Vizcarrondo, G. A., Brown, A. D., and Fogarty, M. J. (2023). Sarcopenia of the longitudinal tongue muscles in rats. *Respir. Physiol. Neurobiol.* 319:104180. doi: 10.1016/j.resp.2023.104180

Slomianka, L. (2020). Basic quantitative morphological methods applied to the central nervous system. *J. Comp. Neurol.* 529, 694–756. doi: 10.1002/cne.24976

Stuesse, S. L., and Fish, S. E. (1984). Projections to the cardioinhibitory region of the nucleus ambiguus of rat. *J. Comp. Neurol.* 229, 271–278. doi: 10.1002/cne.902290211

Sturrock, R. R. (1990). A comparison of age-related changes in neuron number in the dorsal motor nucleus of the vagus and the nucleus ambiguus of the mouse. *J. Anat.* 173, 169–176

Subramanian, H. H., Balnave, R. J., and Holstege, G. (2021). Microstimulation in different parts of the periaqueductal gray generates different types of vocalizations in the cat. *J. Voice* 35, 804.e9–804.e25. doi: 10.1016/j.jvoice.2020.01.022

Subramanian, H. H., Huang, Z. G., Silburn, P. A., Balnave, R. J., and Holstege, G. (2018). The physiological motor patterns produced by neurons in the nucleus retroambiguus in the rat and their modulation by vagal, peripheral chemosensory, and nociceptive stimulation. *J. Comp. Neurol.* 526, 229–242. doi: 10.1002/cne.24318

Sun, Q. J., Pilowsky, P., and Llewellyn-Smith, I. J. (1995). Thyrotropin-releasing hormone inputs are preferentially directed towards respiratory motoneurons in rat nucleus ambiguus. *J. Comp. Neurol.* 362, 320–330. doi: 10.1002/cne.903620303

Thiyagalingam, S., Kulinski, A. E., Thorsteinsdottir, B., Shindelar, K. L., and Takahashi, P. Y. (2021). Dysphagia in older adults. *Mayo Clin. Proc.* 96, 488–497. doi: 10.1016/j.mayocp.2020.08.001

Tomomune, N., and Takata, M. (1988). Excitatory and inhibitory postsynaptic potentials in cat hypoglossal motoneurons during swallowing. *Exp. Brain Res.* 71, 262–272. doi: 10.1007/BF00247486

Turley, R., and Cohen, S. (2009). Impact of voice and swallowing problems in the elderly. *Otolaryngol. Head Neck Surg.* 140, 33–36. doi: 10.1016/j.otohns.2008.10.010

Ulfhake, B., and Cullheim, S. (1988). Postnatal development of cat hind limb motoneurons. III: changes in size of motoneurons supplying the triceps surae muscle. *J. Comp. Neurol.* 278, 103–120

Ulrich, D., Quadroni, R., and Luscher, H. R. (1994). Electronic structure of motoneurons in spinal cord slice cultures: a comparison of compartmental and equivalent cylinder models. *J. Neurophysiol.* 72, 861–871. doi: 10.1152/jn.1994.72.2.861

Umezaki, T., Shiba, K., Zheng, Y., and Miller, A. D. (1998). Upper airway motor outputs during vomiting versus swallowing in the decerebrate cat. *Brain Res.* 781, 25–36. doi: 10.1016/S0006-8993(97)01145-1

Vanderhorst, V. G., Terasawa, E., Ralston, H. J. 3rd, and Holstege, G. (2000). Monosynaptic projections from the lateral periaqueductal gray to the nucleus retroambiguus in the rhesus monkey: implications for vocalization and reproductive behavior. *J. Comp. Neurol.* 424, 251–268. doi: 10.1002/1096-9861(20000821)424:2<251::AID-CNE5>3.0.CO;2-D

Veerakumar, A., Yung, A. R., Liu, Y., and Krasnow, M. A. (2022). Molecularly defined circuits for cardiovascular and cardiopulmonary control. *Nature* 606, 739–746. doi: 10.1038/s41586-022-04760-8

Wetzel, D. M., Kelley, D. B., and Campbell, B. A. (1980). Central control of ultrasonic vocalizations in neonatal rats: I. Brain stem motor nuclei. *J. Comp. Physiol. Psychol.* 94, 596–605. doi: 10.1037/h0077699

Williams, P. A., Bellinger, D. L., and Wilson, C. G. (2019). Changes in the morphology of hypoglossal motor neurons in the brainstem of developing rats. *Anat Rec (Hoboken)* 302, 869–892. doi: 10.1002/ar.23971

Williams, K. P. J., Pitt, G. D., Batchelder, D. N., and Kip, B. J. (1994). Confocal Raman microspectroscopy using a stigmatic spectrograph and Ccd detector. *Appl. Spectrosc.* 48, 232–235. doi: 10.1366/0003702944028407

Zheng, Y., Umezaki, T., Nakazawa, K., and Miller, A. D. (1997). Role of pre-inspiratory neurons in vestibular and laryngeal reflexes and in swallowing and vomiting. *Neurosci. Lett.* 225, 161–164. doi: 10.1016/S0304-3940(97)00208-5